Electronic Supplementary Information

Open-Air, Green-Solvent Processed Organic Solar Cells with Efficiency Approaching 18% and Exceptional Stability

*Thi Le Huyen Mai[a,#] Zhe Sun,[a,#] Seoyoung Kim,[a] Seonghun Jeong,[a] Seunglok Lee,[a] Jeewon Park,[a] and Changduk Yang[a,b]**

[a]School of Energy and Chemical Engineering, Perovtronics Research Center, Low Dimensional Carbon Materials Center, Ulsan National Institute of Science and Technology (UNIST), 50 UNIST-gil, Ulju-gun, Ulsan 44919, South Korea.

[b]Graduate School of Carbon Neutrality, Ulsan National Institute of Science and Technology (UNIST), 50 UNIST-gil, Ulju-gun, Ulsan 44919, South Korea.

* Corresponding authors

Email: yang@unist.ac.kr (C. Y.)

Content

1. Materials and Synthesis

For the synthesis of cathode interface materials, all reagents and solvents were acquired from Sigma-Aldrich, Alfa Aesar, Combi-Blocks, and Ambeed, and they were employed without being purified. Dichloromethane (DCM), acetonitrile (ACN), dimethylformamide (DMF), methanol, toluene, triethylamine from Samchun chemical company, and Sigma-Aldrich. PM6, D18, D18-Cl, BTP-eC9, L8-BO and N3 were acquired from Derthon. PDIN, H75 and 1,7-Dibromoperylene-3,4,9,10-tetracarboxylic acid (PDIN-Br_2) were synthesized as previously reported.[1]

Synthesis of 4-bromo-3-fluoro-N,N-dimethylbenzamide (**1**): To a suspension of 4-bromo-3-fluorobenzoic acid (5.0 g, 22.83 mmol) in DCM (50 mL) was added $SOCl_2$ (3.20 mL) and DMF (0.25 mL) at 10-15 ℃. Then the reaction mixture was heated at 80 ℃ for 2 h. Then, the reaction mixture was concentrated, and the residue was diluted with anhydrous toluene (25 mL) and concentrated in turn for 3 times to remove most of $SOCl_2$. Next, the residue was dissolved in anhydrous DCM (50 mL) at 0 ℃ and added dropwise dimethylamine (30 mL) and triethylamine (12 mL). After the completion of the addition, the reaction mixture was stirred over night at room temperature. The reaction mixture was extracted with DCM. The combined organic layer was washed with aqueous 1M HCl, aqueous NaOH, brine, and dried over anhydrous $MgSO_4$ and concentrated to give (**1**) as the yellow solid (4.78 g, 85% yield). ^{1}H NMR (400 MHz, $CDCl_3$, δ): 7.69 (dd, *J* = 8.2 Hz, 1H), 7.28 (dd, *J* = 8.6 Hz, 1H), 7.17 (ddd, *J* = 8.2 Hz, 1H), 3.19 (d, 6H)

Synthesis of 3-fluoro-N,N-dimethylbenzamide-4-boronic acid pinacol ester (**2**): **1** (4.0 g, 16.25 mmol), [1,1'-Bis(diphenylphosiphino)ferrocene]dichloropalladium(II),complex with DCM (0.66 g, 0.81 mmol), potassium acetate (4.78 g, 48.76 mmol), Bis(pinacolato)diboron (6.27 g, 24.69 mmol) were dissolved in 120 mL of 1,4- dioxane and then the mixture was stirred at 100 °C for 24 h under argon atmosphere. After cooling down to room temperature, the crude mixture was extracted with ethyl acetate, washed with water, brine. Next, solvents were evaporated under reduced pressure after the combined organic layer was dried with anhydrous $MgSO_4$. Consequently, the residue was purified by column chromatography on silica gel (ethyl acetate : hexane = 4:1) to obtain **2** as the off-white solid (4.52 g, 95% yield). ^{1}H NMR (400 MHz, $CDCl_3$, δ):, 7.77 (dd, *J* = 7.6 Hz, 1H), 7.18 (dd, *J* = 7.5 Hz, 1H), 7.07 (dd, *J* = 9.2 Hz, 1H), 3.10 (s, 3H), 2.94 (s, 3H), 1.36 (s, 12H).

Synthesis of 4-bromo-2,5-difluoro-N,N-dimethylbenzamide (**3**): Synthesized according to a similar procedure to compound **1** by utilizing 4-Bromo-2,5-difluorobenzoic acid (5.0 g, 21.09 mmol), $SOCl_2$ (2.71 mL), DMF (0.25 mL), DCM (50 mL), dimethylamine (30 mL) and triethylamine (12 mL), DCM (50 mL). (**3**) as yellow solid (5.27 g, 95% yield). ^{1}H NMR (400 MHz, $CDCl_3$, δ): 7.34 (dd, *J* = 8.0 Hz, 1H), 7.16 (dd, *J* = 7.8 Hz, 1H), 3.12 (s, 3H), 2.94 (s, 3H).

Synthesis of 2,5-difluoro-N,N-dimethylbenzamide-4-borobic acid pinacol ester (**4**): Synthesized according to a similar procedure to compound **2** by utilizing **3** (5.2 g, 19.69 mmol), [1,1'-Bis(diphenylphosiphino)ferrocene]dichloropalladium(II),complex with DCM (0.60 g, 0.73 mmol), potassium acetate (5.79 g, 58.99 mmol), Bis(pinacolato)diboron (7.50 g, 29.53 mmol) and 1,4-dioxane (120 mL). (**4**) as off-white solid (5.80 g, 95% yield). ^{1}H NMR (400 MHz, $CDCl_3$, δ): 7.42 (dd, *J* = 8.8 Hz, 1H), 7.04 (dd, *J* = 8.0 Hz, 1H), 3.11 (s, 3H), 2.91 (s, 3H), 1.35 (s, 12H).

Synthesis of H75-2F: PDIN-Br_2 (1.0 g, 1.39 mmol), **2** (1.22 g, 4.16 mmol), potassium carbonate (3.84 g, 27.80 mmol) and Pd(pph3)4 (0.08 g, 0.06 mmol) was dissolved in 120 mL/60 mL/30 mL toluene/ethanol/water. Then, the mixture reaction was stirred at 100 °C for 24 h under the argon atmosphere. After cooling down to room temperature, the crude mixture was extracted with chloroform, washed with water, brine. Next, solvents were evaporated under reduced pressure after the combined organic layer was dried with anhydrous MgSO4. The residue was purified by column chromatography on silica gel (chloroform : triethylamine : methanol =4.0:0.2:0.2) to obtain **H75-2F** as the red solid (0.99 g, 80%). ^{1}H NMR (400 MHz, $CDCl_3$, δ): 8.68 (m, 4H), 8.55 (s, 0.5H), 8.25 (dd, *J* = 8.0 Hz, 1H), 7.98 (m, 2H), 7.77 (t, 0.5H), 7.66 (t, 0.5H), 7.58 (t, 0.5H), 7.51 (m, 1H), 7.41 (m, 0.5H), 7.36 (m, 0.5H), 7.30 (m, 0.5H), 7.23 (m, 0.5H), 4.23 (m, 4H), 3.18 (d, 12H), 2.44 (m, 4H), 2.27 (s, 12H), 1.9 (m, 4H). ^{13}C NMR (151 MHz, CDCl3, δ): 169.24, 163.13, 139.07, 135.95, 135.41, 135.06, 134.73, 134.23, 133.99, 133.57, 133.35, 133.19, 132.89, 131.29, 130.90, 130.42, 130.15, 128.91, 128.66, 128.53, 128.03, 127.06, 125.12, 124.80, 123.69, 123.33, 123.06, 122.73, 122.55, 116.09, 62.69, 57.20, 45.38, 39.68, 39.00, 35.57, 29.70, 26.08. .HRMS (MALDI-TOF): calcd for $C52H48F_2N6O6$, 890.99. Found: 891.37.

Synthesis of H75-4F: Synthesized according to a similar procedure to H75-1F by utilizing PDIN Br_2 (1.0 g, 1.39 mmol), **4** (1.30 g, 4.18 mmol), potassium carbonate (3.84 g, 27.80 mmol) and Pd(pph3)4 (0.08 g, 0.06 mmol) and toluene/ethanol/water (120 mL/60 mL/30 mL). **H75-4F** as

dark red solid (0.96 g, 75% yield). ^{1}H NMR (400 MHz, $CDCl_3$, δ): 8.69 (m, 3H), 8.59 (d, J = 5.9 Hz, 0.5H), 8.53 (s, 0.5H), 8.33 (dd, J = 8.1 Hz, 2H), 8.00 (dd, J = 8.3, 2H), 7.49 (m, 0.5H), 7.38 (m, 0.5H), 7.31 (m, 0.5H), 7.20 (m, 0.5H), 4.26 (m, 4H), 3.20 (s, 6H), 3.08 (s, 6H), 2.46 (m, 4H), 2.27 (s, 11H), 1.93 (m, 4H). ^{13}C NMR (151 MHz, CDCl3, δ): 169.24, 163.13, 139.07, 135.95, 135.41, 135.06, 134.73, 134.23, 133.99, 133.57, 133.35, 133.19, 132.89, 131.29, 130.90, 130.42, 130.15, 128.91, 128.66, 128.53, 128.03, 127.06, 125.12, 124.80, 123.69, 123.33, 123.06, 122.73, 122.55, 116.09, 62.69, 57.20, 45.38, 42.50, 39.68, 39.00, 36.71, 35.57, 31.93, 29.70, 26.08, 25.73, 22.70. HRMS (MALDI-TOF): calcd for $C_{52}H_{46}F_4N_6O_6$, 926.97. Found: 927.34.

2. Instruments and Characterizations

^{1}H NMR spectra were determined on a 400 MHz FT-NMR (Bruker) (AVANCE III HD) spectrometer using deuterated chloroform solution ($CDCl_3$) as solvent at 298 K. ^{13}C NMR spectra were investigated on a 600 MHz FT-NMR (Bruker) (AVANCE NEO) spectrophotometer using $CDCl_3$. A Shimadzu UV-2550 spectrometer was used to obtain UV-vis spectra. An AMETEK Versa STAT 3 equipped with a three-electrode cell system was used to measure cyclic voltammetry (CV) at room temperature using a nitrogen-bubbled 0.1 M tetra-n-butylammonium hexafluorophosphate (n-Bu_4NPF_6) in acetonitrile (CH_3CN) solution at a scan rate of 100 mV^{-1} s^{-1}. As the reference electrode, counter electrode, and working electrode, respectively, Ag/Ag^{+}, platinum wire, and glassy carbon electrode were used. An autoflex max instrument (Bruker) was used to measure the results of the MALDI-TOF mass spectrometry experiments. Thermogravimetric Analysis (TGA) were measured using Q500 (TA instruments, USA) with a scan rate of 10 °C per minute in nitrogen flow.

Employing ultraviolet photoelectron spectra (UPS) and high-resolution XPS scans, the ESCALAB 250XI analyzer from Thermo Fisher Scientific was employed to determine the films' work function and atom concentration distribution. EMXplus (Bucker) (300 K, 9.3~9.9 GHz, X-band, microwave maximum source output 200 mW) was used to record Electron Spin Resonance Spectrometer (ESR) spectra. The results of TOF-SIMS 5 (ION TOF) were obtained using time of flight secondary ion mass spectrometry (TOF-SIMS).

Multimode V microscope (Veeco, USA) was used to carried out the microscopy surface of the thin films with a nanscope controller using Si tips (Bruker) for atomic force microscopy (AFM) images and Pt:Ti-coated tips (SPARK 70 Pt, Nu Nano Ltd) for surface potential measurements (KPFM). GIWAXS was conducted at the Pohang Accelerator Laboratory in Korea at the PLS-II 6D U-SAXS and 9A beamline. A Rayonix SX165 two-dimensional CCD detector was used to record the scattering signal. The energy of the X-ray light was 11.24 KeV. The X-ray incidence angle was set between 0.08 and 0.12 in order to optimize the signal-to-background ratio.

The contact angles were measured using a goniometer (DSA100, KRÜSS, Germany) at ambient temperature. For the contact angle measurements of water on CIM film surfaces, 6 µL water was dropped onto each of H75, H75-2F, and H75-4F neat films. For the contact angle measurements of CIM solutions on the active layer, 6 µL droplets of H75, H75-2F, H75-4F and PDIN were dropped onto the surface of active layer. The average values were obtained from at least three measurements.

3. Device Fabrication and Characterization

The organic solar cell devices were fabricated with conventional architecture ITO/PEDOT : PSS/active layer/cathode interface material (CIM)/Ag. The ITO glasses were sequentially washed with detergent, deionized water, acetone, and isopropyl alcohol under sonication system and then dried overnight in an oven. After being treated by UV-Ozone for 20 min, PEDOT:PSS (Bayer Baytron 4083) was spin-coated at 4000 rpm onto ITO glasses (~ 30 nm), followed by annealing at 150 °C for 20 min in air. Next, the blend solution of PM6 : BTP-eC9 (1.0 : 1.2) in o-xylene at 21 mg/mL was spin-coated at 2200 rpm onto the PEDOT: PSS layer, and then the active layers were annealed at 80 °C for 10 min. In the case of D18/L8-BO, D18 was dissolved in chlorobenzene at a concentration of 4 mg/ml and spin-coated at 1600 rpm. Subsequently, L8-BO dissolved in chloroform at 10mg/mL was spin-coated at 3000rpm. And annealing at 100 °C for 2 min. In the case of D18-Cl : N3 system, the blend solution of D18-Cl:N3 (1.0 : 1.4) in CF at 10 mg/mL was spin-coated at 2200 rpm before annealing at 80 °C for 10 min. DIB at 60% mass fraction as additive. In case of PM6:Y6 system, the blend solution of PM6:Y6 (1.0 : 1.2) in CF at 15.5mg/mL was spin-coated at 2700 rpm before annealing at 80 °C for 5 min. CN at 0.5% volume fraction as additive.

After that, the ethanol solution of H75 (2.0 mg/mL), H75-1F (2.0 mg/mL), H75-2F (0.5 mg/mL) or PDIN (2.0 mg/mL, 1.5% acid acetic) was spin-coated onto the active layer with 3000 rpm for 30s. Finally, Ag cathode (~ 100nm) was thermally evaporated on top of the substrates under high vacuum (<3.0 x 10-6 Pa).

Relevant to the fabrication of air-processed OSCs, all processes from making the blend solution of PM6:BTP-eC9 active layer, annealing and spin-coating the cathode interface layer were conducted in ambient environment in high humidity conditions (RH of 60%–80%). The temperature was controlled at 25±3°C.

Under the light of an AM 1.5G solar simulator, current density–voltage (*J*–*V*) measurements were made using a Keithley 2400 source–measure unit at an intensity of 100 mW cm^{-2}. A standard Si solar cell was used to calibrate the light intensity of the solar simulator. The external quantum efficiency (EQE) measurements were conducted using Model QE-R3011 (Enli Technology) in ambient air. SCLC method was used to measure the electron mobilities through ITO/ZnO/CIM/Al. And the SCLC mobilities were calculated using the Mott–Gurney equation, $J_{SCLC} = (9/8)\varepsilon_0\varepsilon_r\mu((V^2)/(L^3))$, where εr is the relative dielectric constant of the organic semiconductor, ε0 is the permittivity of empty space, μ is the mobility of zero-field, L is the thickness of the active layer, and V is applied voltage across the device. The electrochemical impedance spectroscopy (EIS) measurement was performed using a E4990A Impedance Analyzer with a 20 mV ac signal at frequencies from 5 MHz to 20 Hz under the dark. A bias voltage equal to *V*oc was applied to offset the total current. Using the analyzer function of an organic semiconductor parameter test system (McScience T4000), transient photovoltage (TPV) transient photocurrent (TPC) measurements were carried out in the presence of a white light-emitting diode.

4. Conductivity and Electron Mobility Measurement

CIMs in chloroform were spin-coated at a film thickness (d) of ~100 nm on substrates with parallel silver electrodes and the conductivities of the CIMs were measured by the slope of the I–V plot using the equation $I = \sigma \times A \times V \times d^{-1}$, where d is the film thickness and A is the sample area. To assess charge transport and extraction efficiency, electron mobility of H75 derivatives was

quantified using the space-charge-limited current (SCLC) method in electron-only devices (ITO/ZnO/CIM/Al).

5. Stability Measurement

The PM6:BTP-eC9 system was employed to conduct long-term thermal, light-soaking, and air stability testing on unencapsulated devices. Cells were placed on petri plates and stored in a nitrogen-filled glovebox for long-term stability testing. To test thermal stability, cells were placed on a hot plate at 85 °C in a glovebox filled with nitrogen and covered with aluminum foil to block room light. The PCE was occasionally recorded after cooling at ambient temperature. To assess light-soaking stability, the cells were exposed to 100 mW cm^{-2} continuous illumination in a nitrogen-filled glovebox utilizing ORIEL LED Solar Simulator (LSH7320 ABA). Using room light, the cells were tested for air stability at 25 °C and 40%–60% RH.

6. Figures and Tables

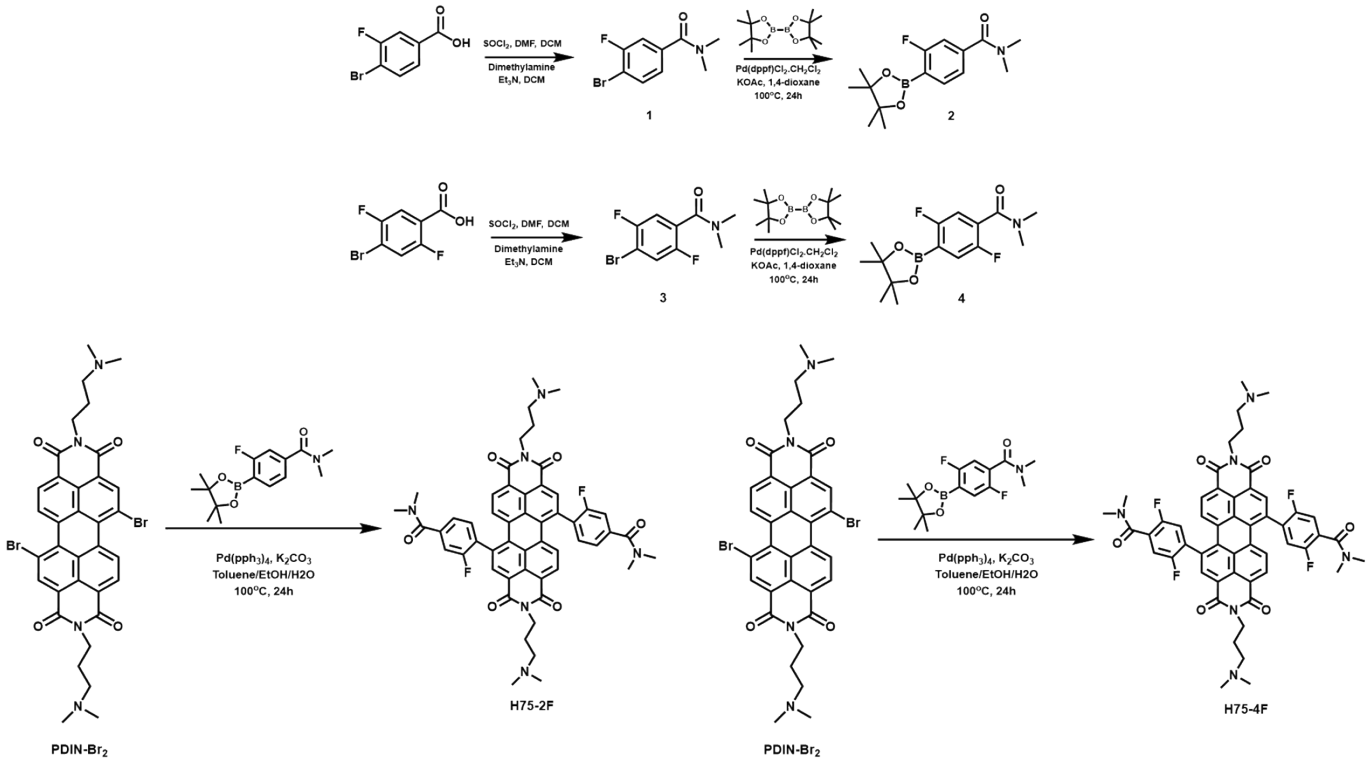

Fig. S1 The synthetic route of H75-2F and H75-4F.

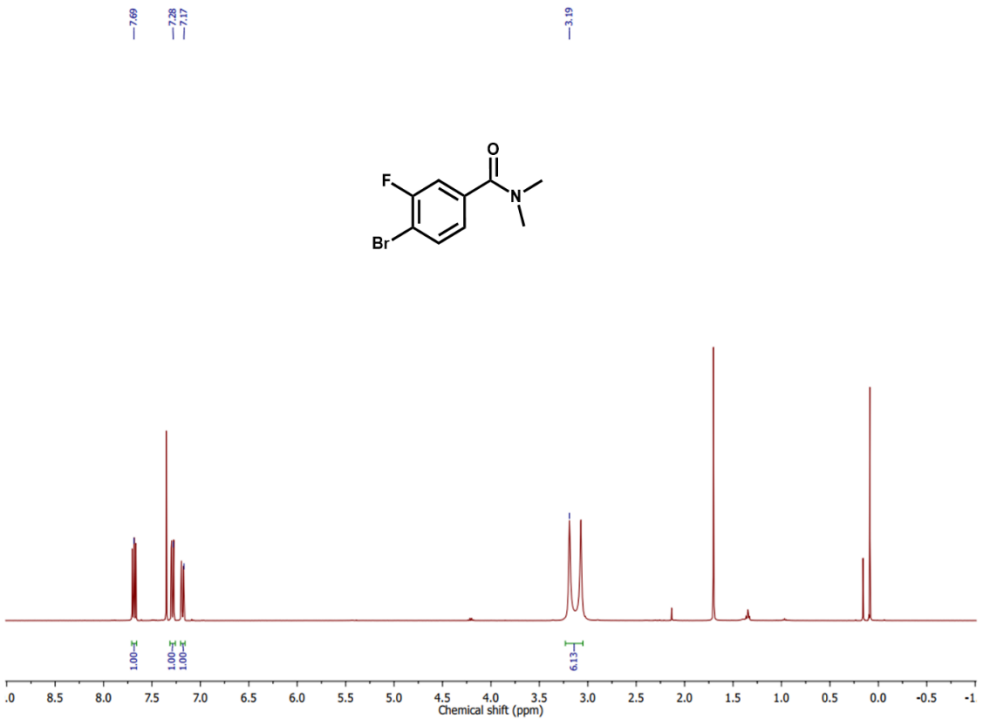

Fig. S2 ^{1}H NMR spectrum of 4-bromo-3-fluoro-*N,N*-dimethylbenzamide.

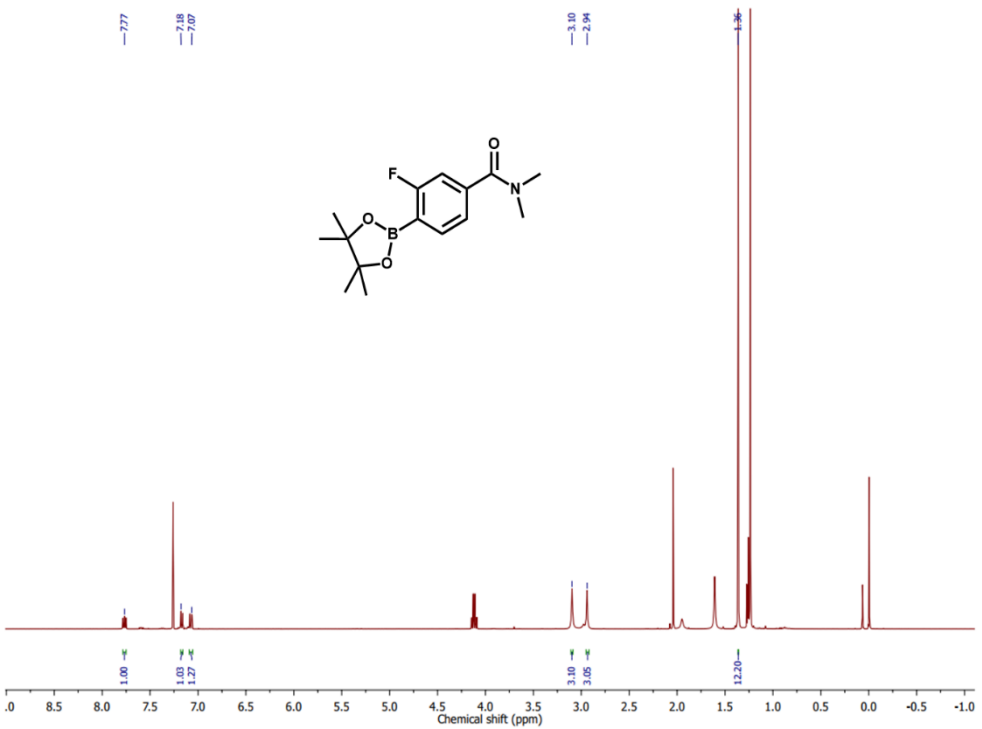

Fig. S3 ^{1}H NMR spectrum of 3-fluoro-*N,N*-dimethylbenzamide-4-boronic acid pinacol ester.

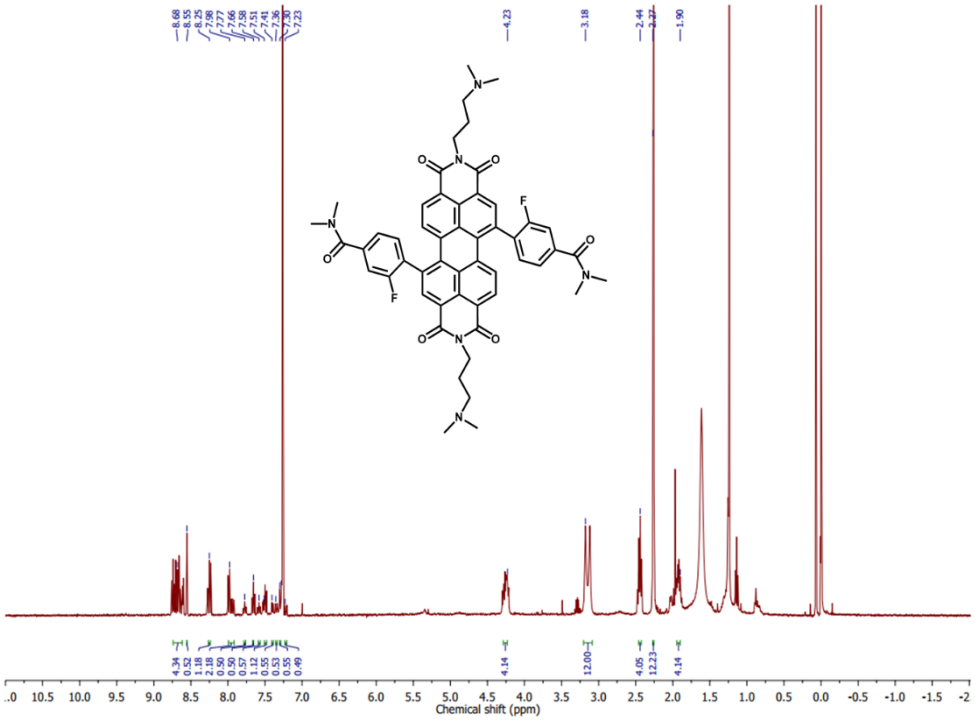

Fig. S4 ^{1}H NMR spectrum of H75-2F.

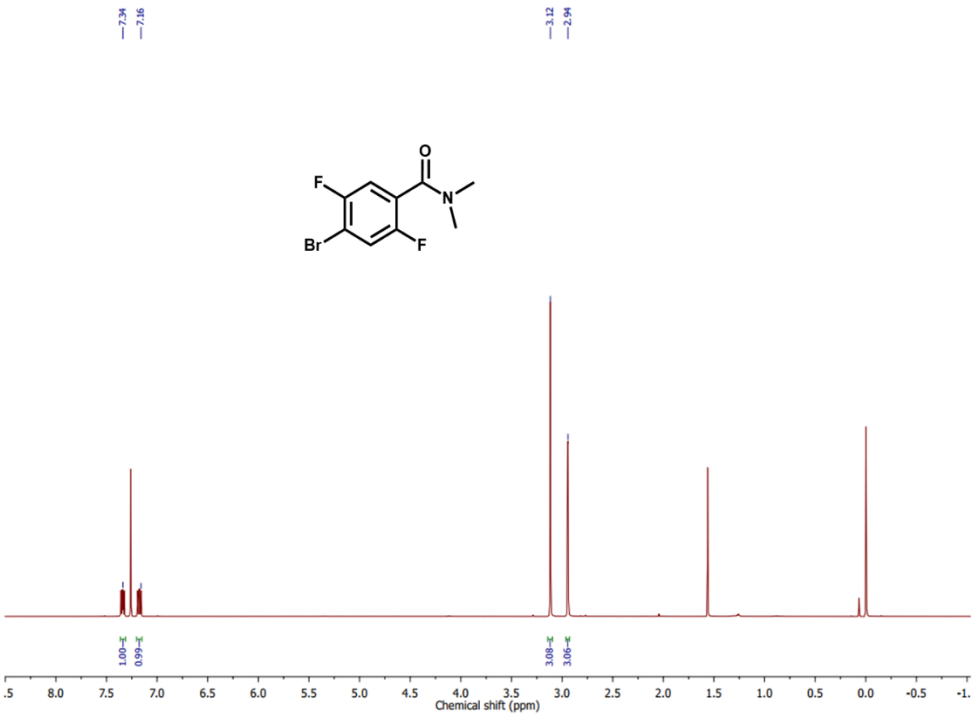

Fig. S5 ^{1}H NMR spectrum of 4-bromo-2,5-difluoro-*N,N*-dimethylbenzamide.

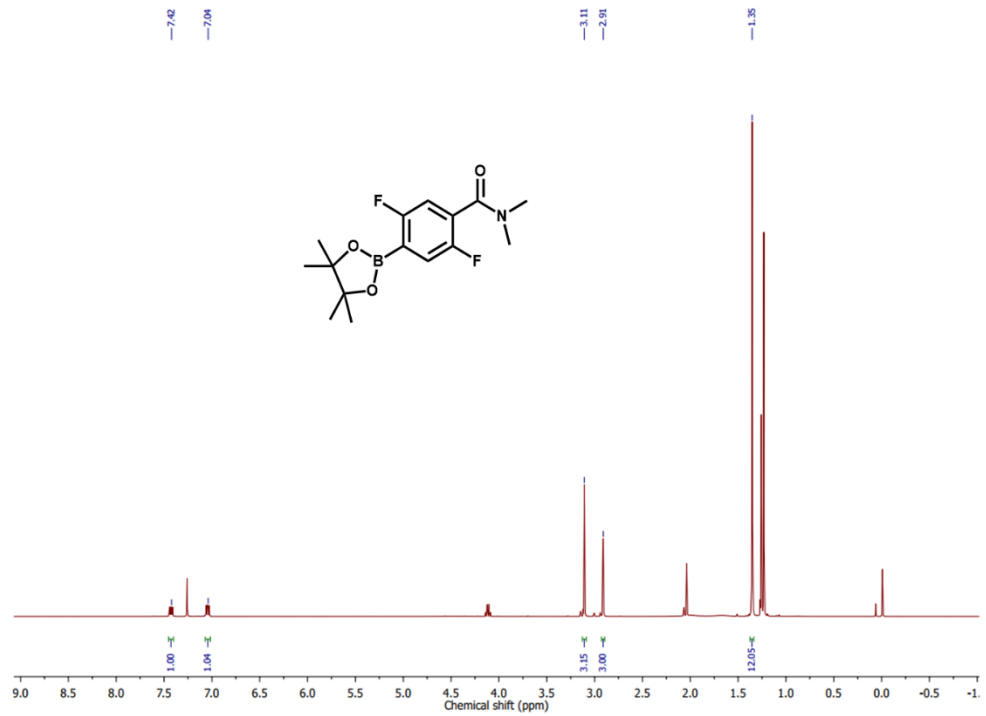

Fig. S6 ^{1}H NMR spectrum of 2,5-difluoro-*N,N*-dimethylbenzamide-4-borobic acid pinacol ester.

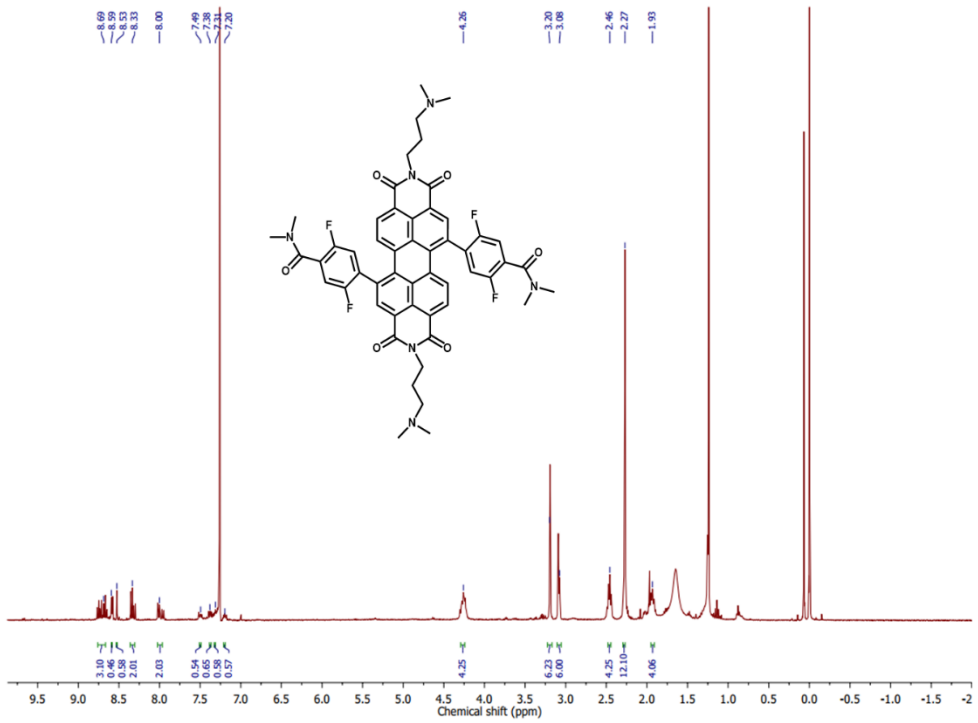

Fig. S7 ^{1}H NMR spectrum of H75-4F.

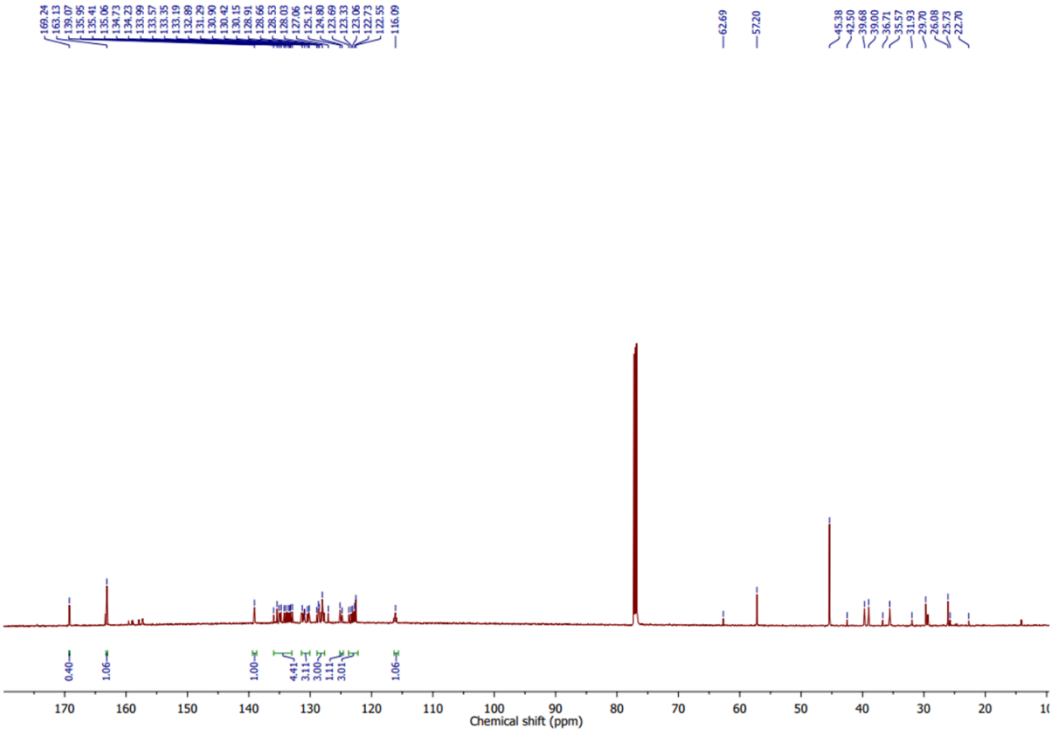

Fig. S8 The integrated ^{13}C NMR spectrum of H75-2F.

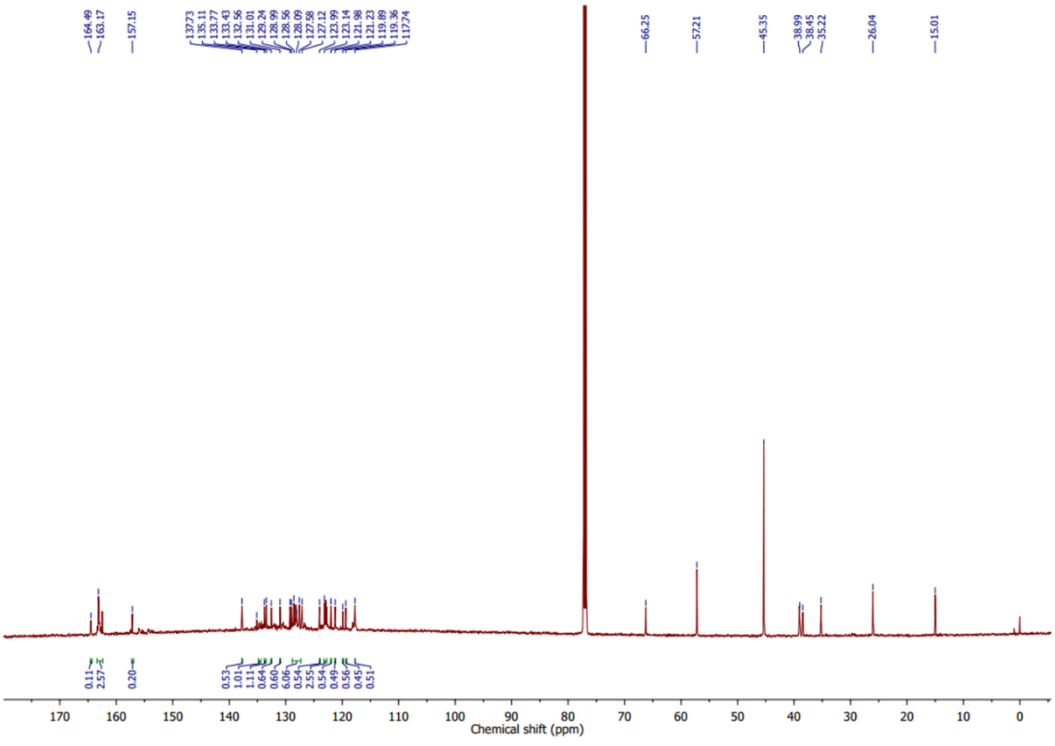

Fig. S9 The integrated ^{13}C NMR spectrum of H75-4F.

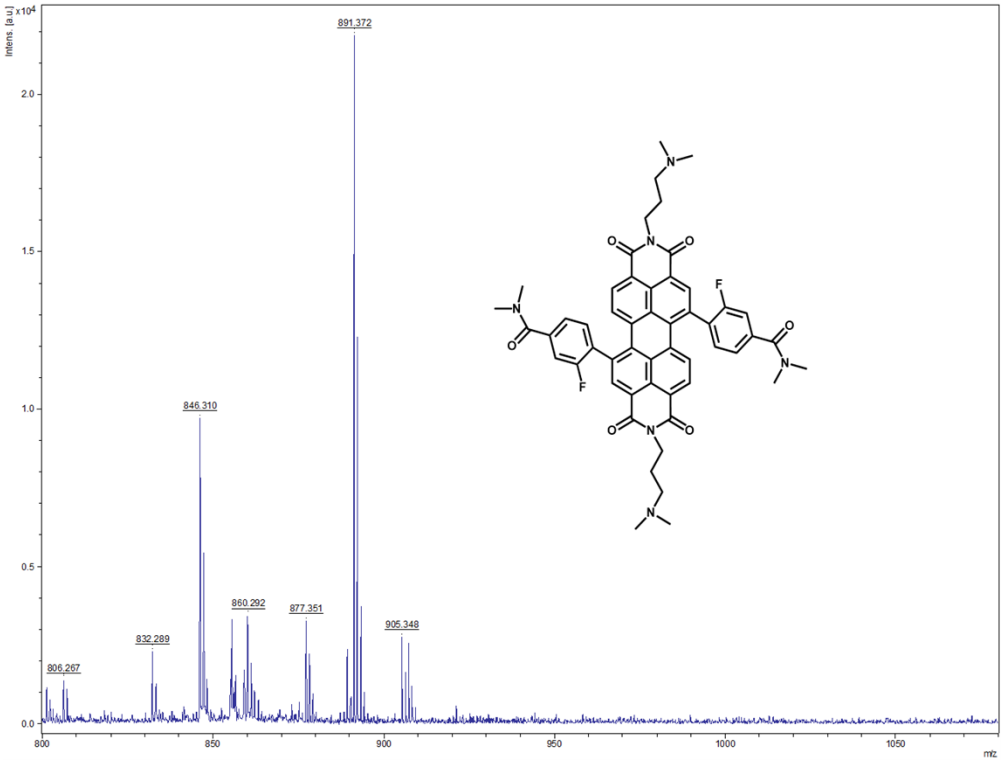

Fig. S10 MALDI-TOF mass spectrometry of H75-2F.

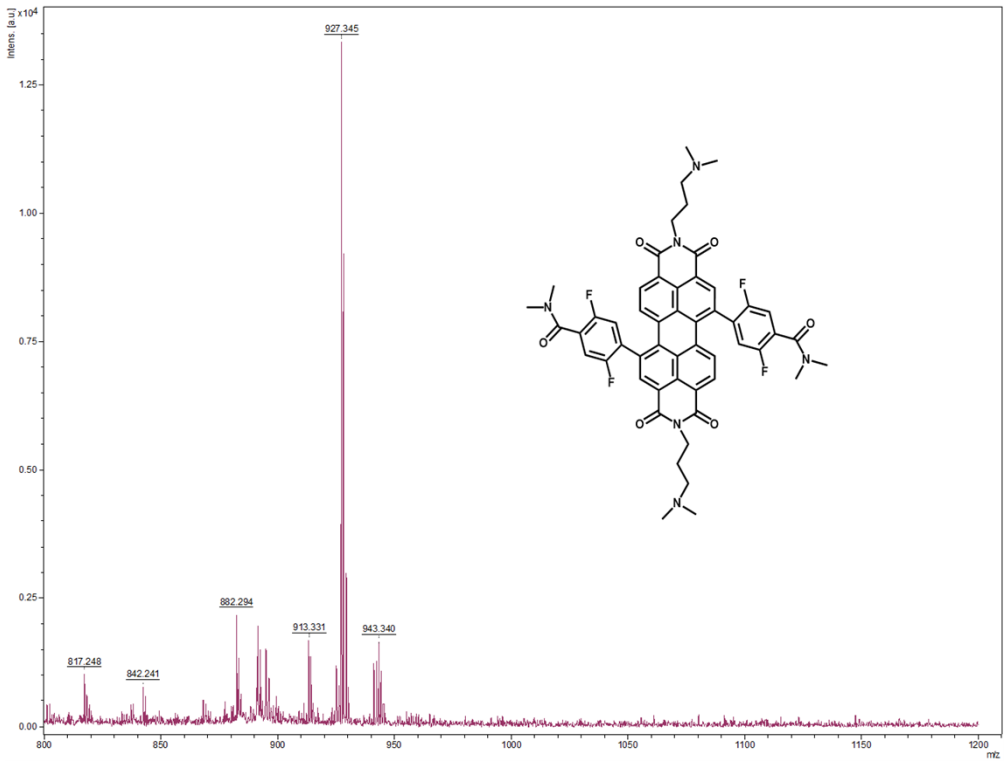

Fig. S11 MALDI-TOF mass spectrometry of H75-4F.

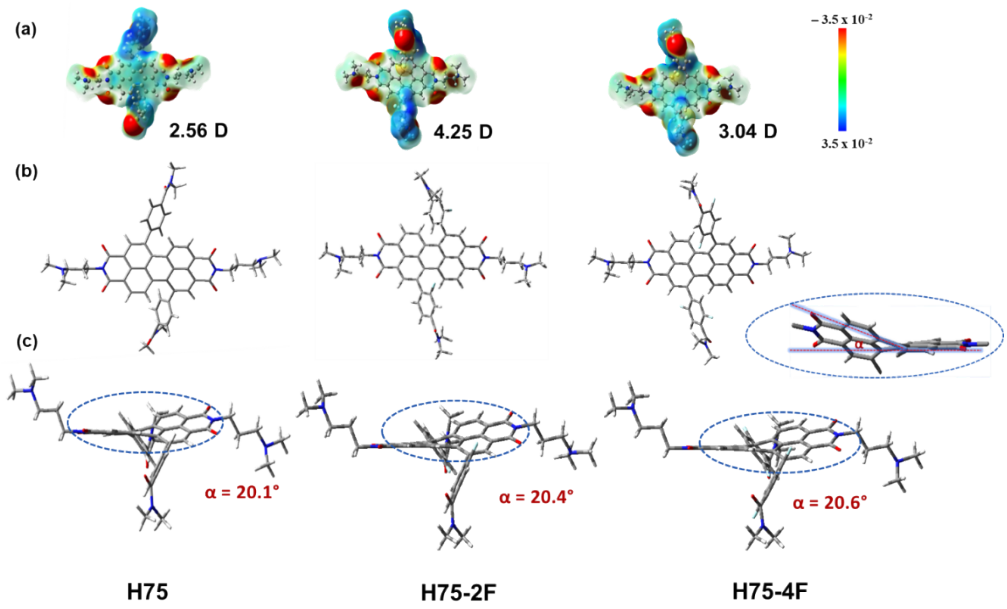

Fig. S12 Geometries are optimized by B3LYP/6-31G levels.(a) Electrostatic potential (ESP) distribution and dipole moment,(b) In front of view and (c) Side view of H75,H75-2F, and H75-4F.

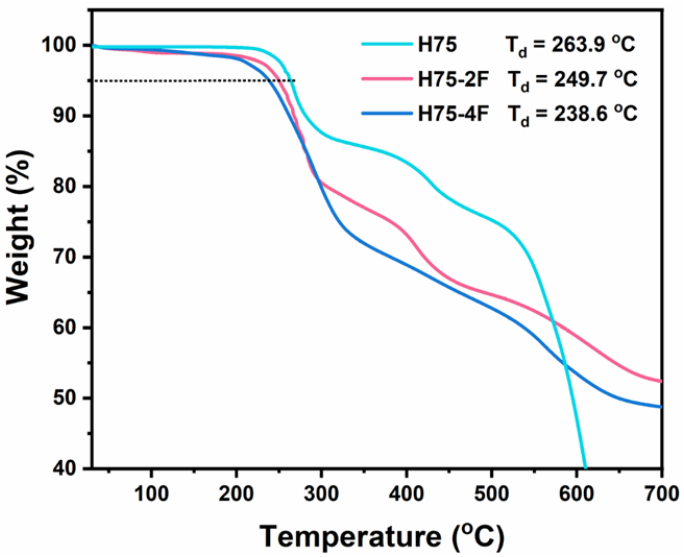

Fig. S13 TGA plots of H75, H75-2F, and H75-4F.

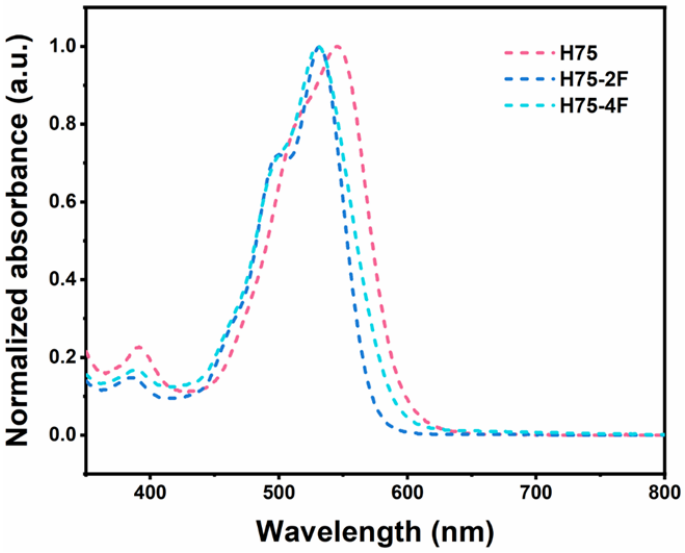

Fig. S14 Normalized UV–vis absorption spectra of H75, H75-2F, and H75-4F in ethanol solution.

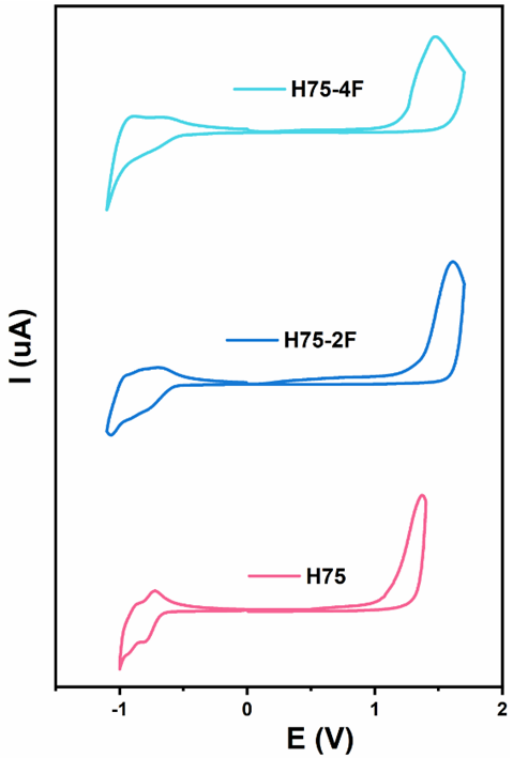

Fig. S15 Cyclic voltammograms of H75, H75-2F, and H75-4F films in acetonitrile solution.

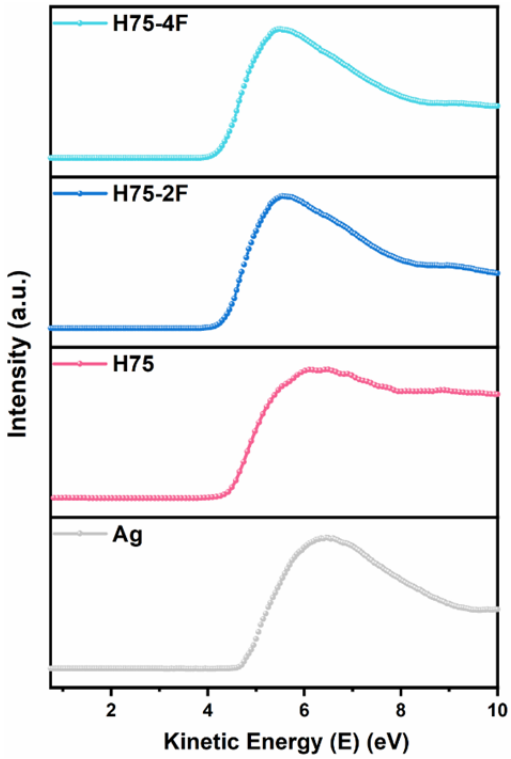

Fig. S16 UPS spectra of the Ag electrodes covered with H75, H75-2F, and H75-4F-based CIMs.

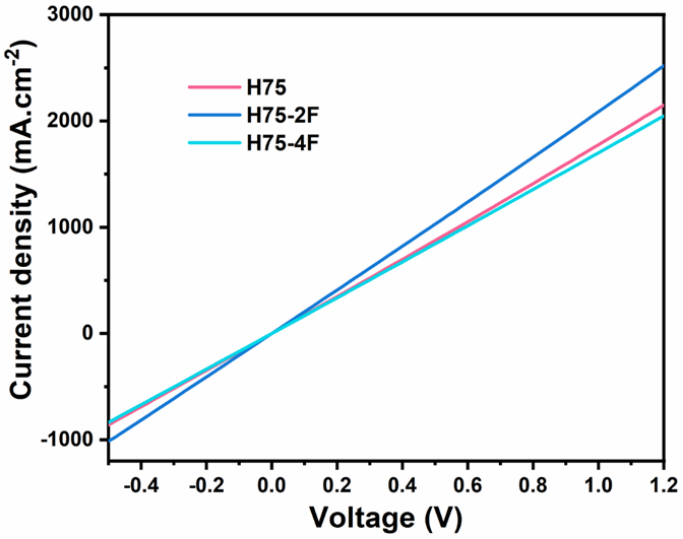

Fig. S17 The *J*–*V* curve of devices with configuration of ITO/CIM/Ag.

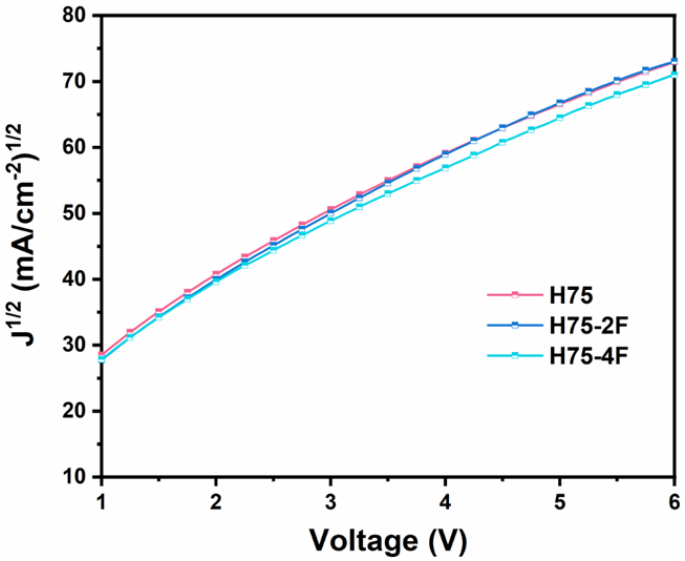

Fig. S18 SCLC plots of electron only devices with the configuration of ITO/ZnO/CIM/Al.

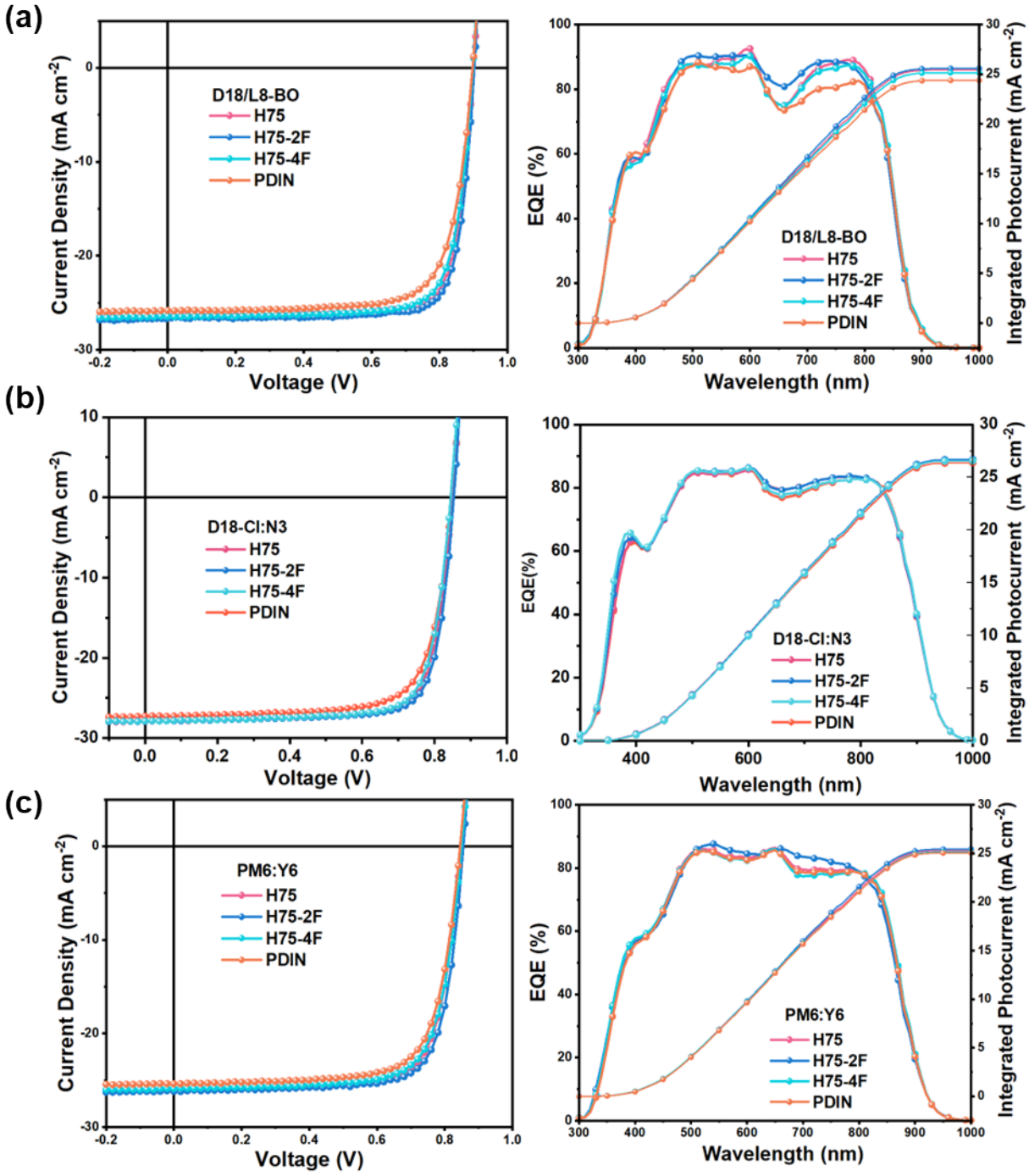
(a)
Current Density (mA cm-2)
Voltage (V)
D18/L8-BO
H75
H75-2F
H75-4F
PDIN
EQE (%)
Integrated Photocurrent (mA cm-2)
Wavelength (nm)
(b)
D18-Cl:N3
EQE(%)
(c)
PM6:Y6

Fig. S19 The *J*-*V* curves and EQE spectra of the devices based on a) D18/L8-BO, b)D18-Cl:N3, c) PM6:Y6 system with H75, H75-2F, H75-4F, and PDIN CIMs.

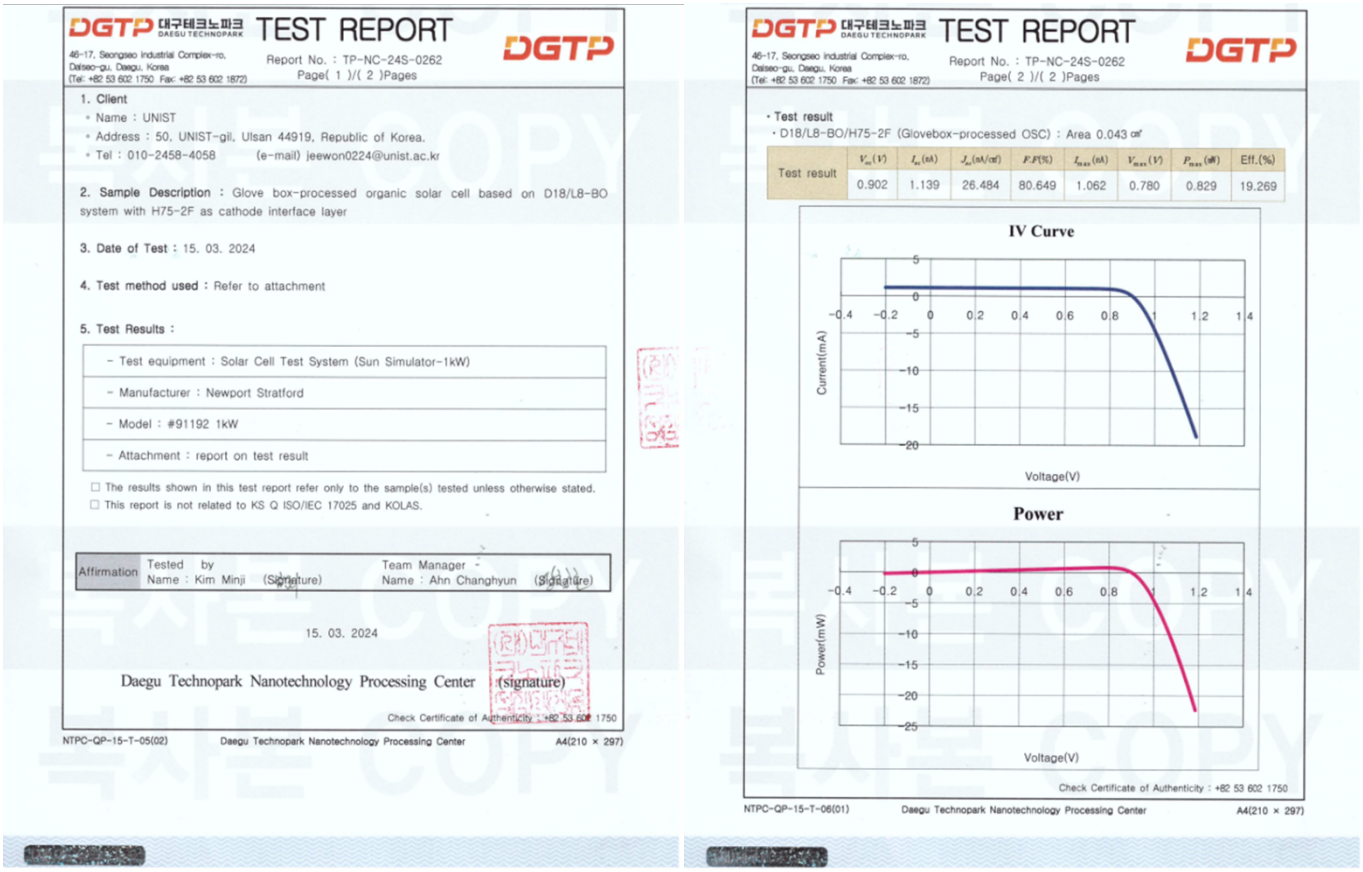

Fig. S20 Certificate of glovebox-processed organic solar cell based on D18/L8-BO system with H75-2F as cathode interface layer from Deagu Technopark Nanotechnology Processing Center (DGTP), Daegu, Korea.

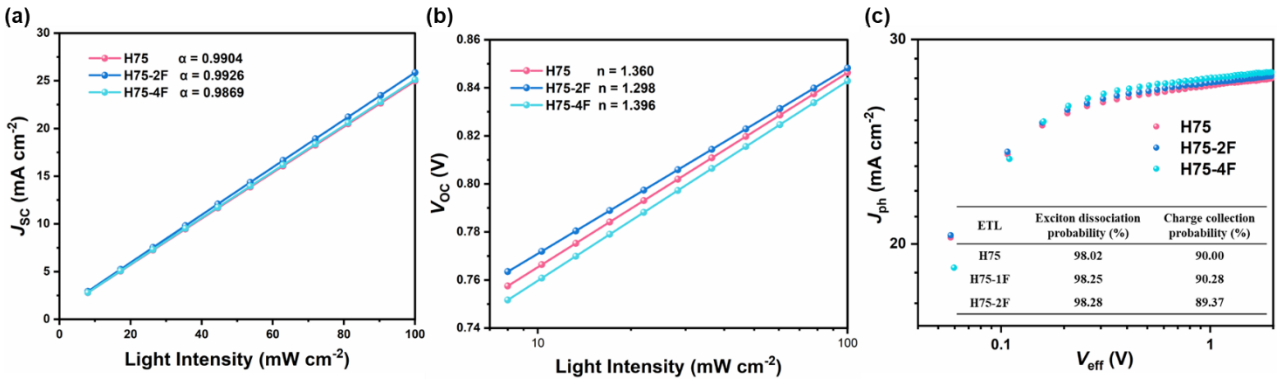

Fig. S21 (a–b) Light intensity dependence of J_{SC} and V_{OC} and c) J_{ph} versus V_{eff} plots of the optimized OSCs with H75, H75-2F and H75-4F CIMs based on PM6:BTP-eC9 system.

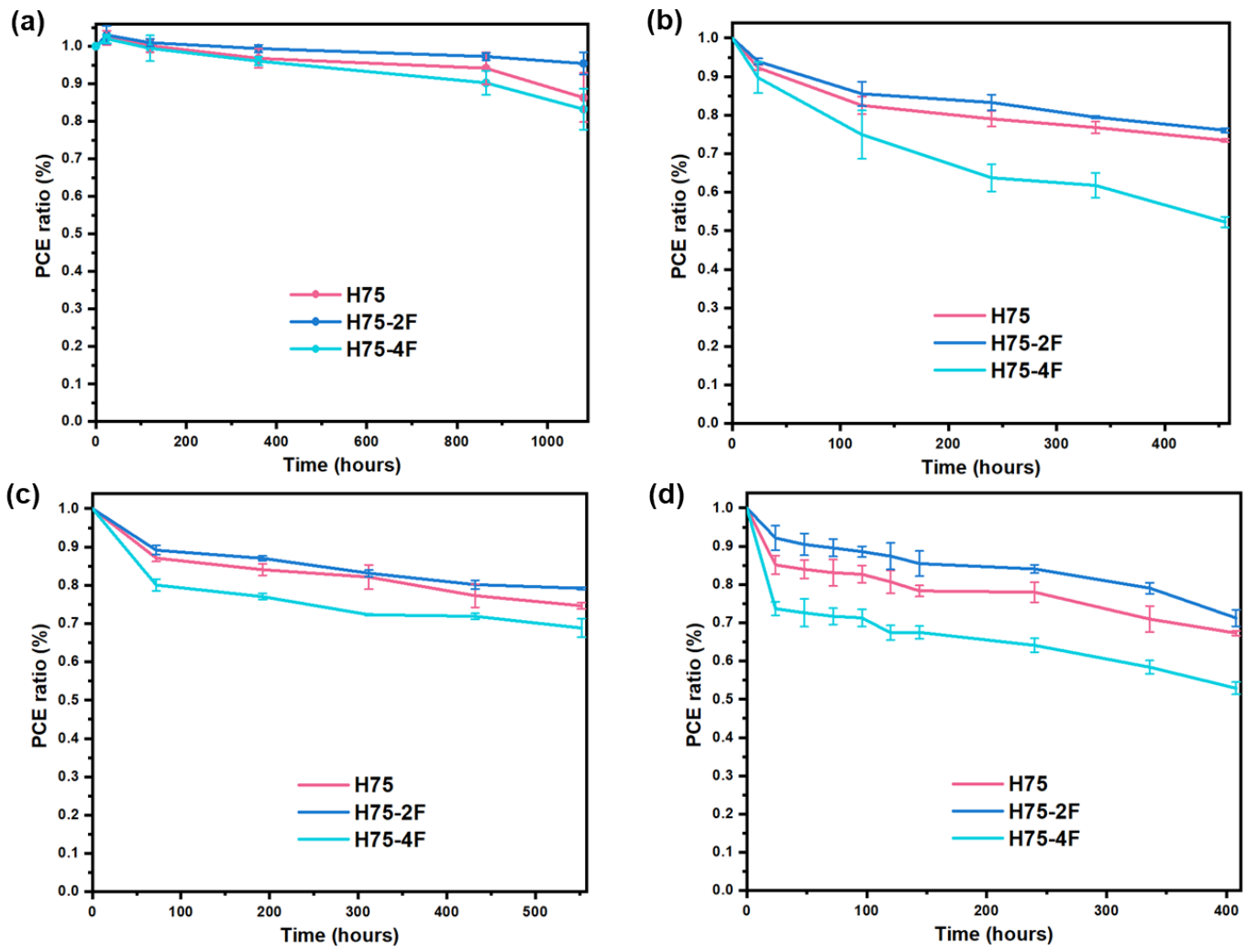

Fig. S22 Normalized average PCEs of the unencapsulated OSC devices with H75, H75-2F, and H75-4F as a function of time according to the different conditions: under a) glovebox (long-term stability), b) thermal stress at 85 °C (thermal stability), c) ORIEL LED solar simulator (light-soaking stability), and d) air ambient environment, 40–60% RH at 25 °C (air stability). The average PCEs and standard variation bars are obtained from 10 individual devices.

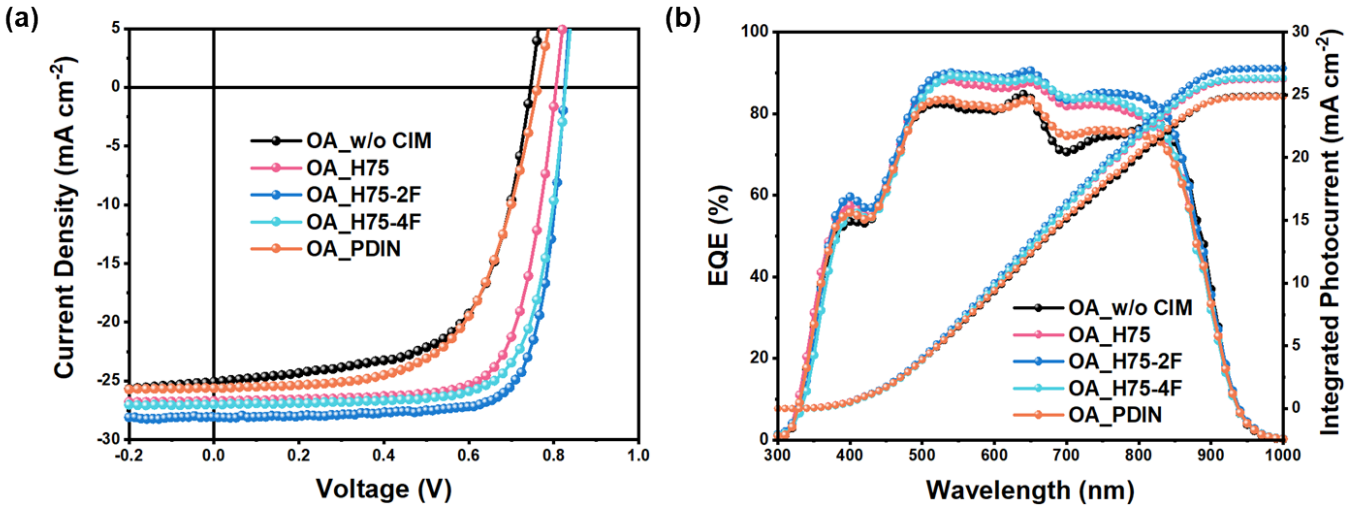

Fig. S23 (a) The *J*–*V* curves of the OA-processed devices without and with H75, H75-2F, H75-4F, and PDIN CIMs under the illumination of AM 1.5G. (b) The EQE spectra and integrated current densities of the devices.

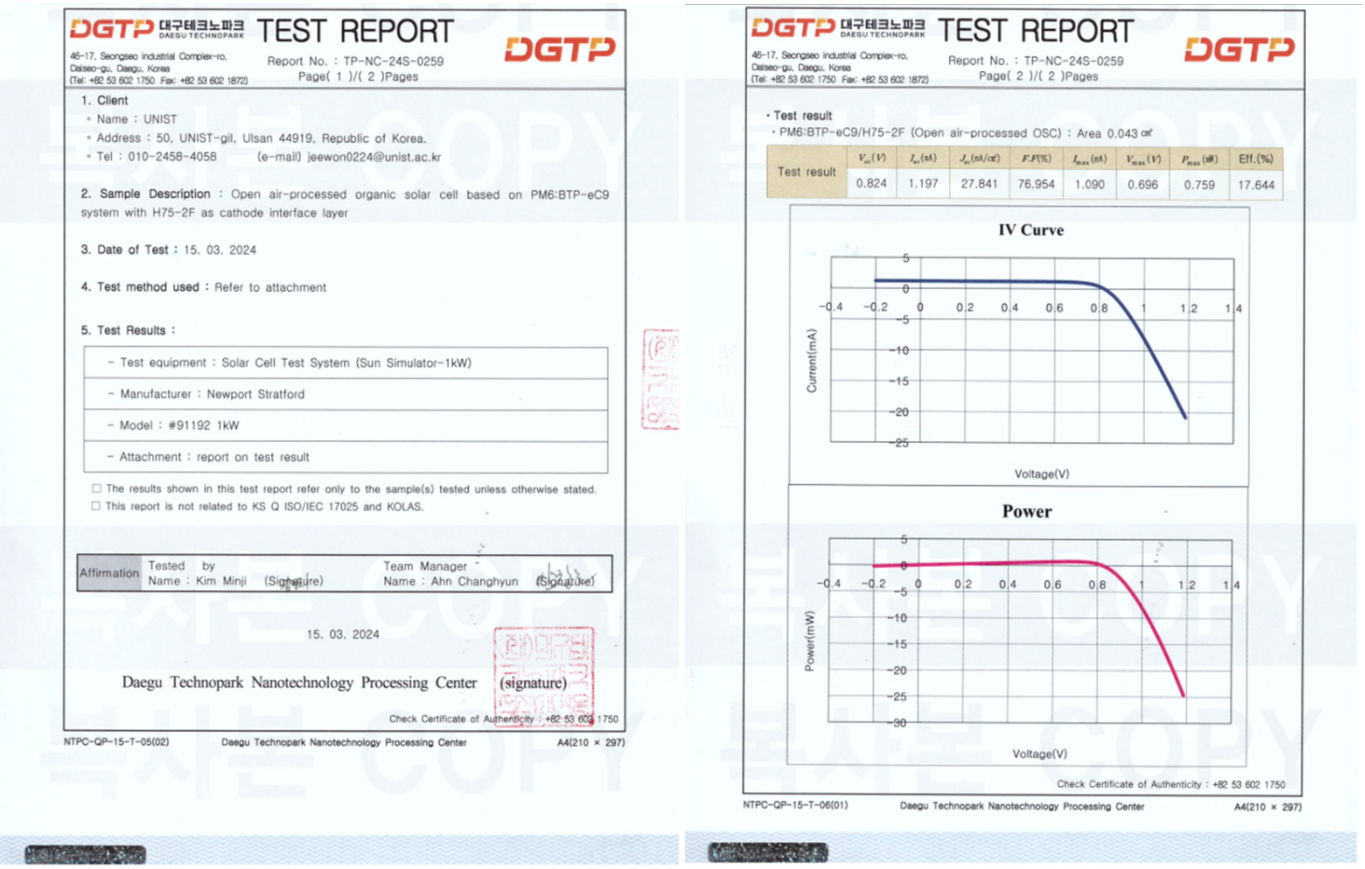

DGTP 대구테크노파크 DAEGU TECHNOPARK TEST REPORT DGTP

46-17, Seongseo industrial Complex-ro, Daiseo-gu, Daegu, Korea (Tel: +82 53 602 1750 Fax: +82 53 602 1872)

Report No. : TP-NC-24S-0259

Page(1)/(2)Pages

1. Client
- Name : UNIST
- Address : 50, UNIST-gil, Ulsan 44919, Republic of Korea.
- Tel : 010-2458-4058 (e-mail) jeewon0224@unist.ac.kr

2. Sample Description : Open air-processed organic solar cell based on PM6:BTP-eC9 system with H75-2F as cathode interface layer

3. Date of Test : 15. 03. 2024

4. Test method used : Refer to attachment

5. Test Results :

- Test equipment : Solar Cell Test System (Sun Simulator-1kW)
- Manufacturer : Newport Stratford
- Model : #91192 1kW
- Attachment : report on test result

☐ The results shown in this test report refer only to the sample(s) tested unless otherwise stated.
☐ This report is not related to KS Q ISO/IEC 17025 and KOLAS.

Affirmation — Tested by Name : Kim Minji (Signature) — Team Manager Name : Ahn Changhyun (Signature)

15. 03. 2024

Daegu Technopark Nanotechnology Processing Center (signature)

Check Certificate of Authenticity : +82 53 602 1750

NTPC-QP-15-T-05(02) Daegu Technopark Nanotechnology Processing Center A4(210 × 297)

DGTP 대구테크노파크 DAEGU TECHNOPARK TEST REPORT DGTP

46-17, Seongseo industrial Complex-ro, Daiseo-gu, Daegu, Korea (Tel: +82 53 602 1750 Fax: +82 53 602 1872)

Report No. : TP-NC-24S-0259

Page(2)/(2)Pages

• Test result
• PM6:BTP-eC9/H75-2F (Open air-processed OSC) : Area 0.043 ㎠

	V_{oc} (V)	J_{sc} (mA)	J_{sc} (mA/㎠)	F.F(%)	I_{max} (mA)	V_{max} (V)	P_{max} (㎽)	Eff.(%)
Test result	0.824	1.197	27.841	76.954	1.090	0.696	0.759	17.644

IV Curve

Current(mA)

Voltage(V)

Power

Power(mW)

Voltage(V)

Check Certificate of Authenticity : +82 53 602 1750

NTPC-QP-15-T-06(01) Daegu Technopark Nanotechnology Processing Center A4(210 × 297)

Fig. S24 Certificate of open air-processed organic solar cell based on PM6:BTP-eC9 system with H75-2F as cathode interface layer from Deagu Technopark Nanotechnology Processing Center (DGTP), Daegu, Korea.

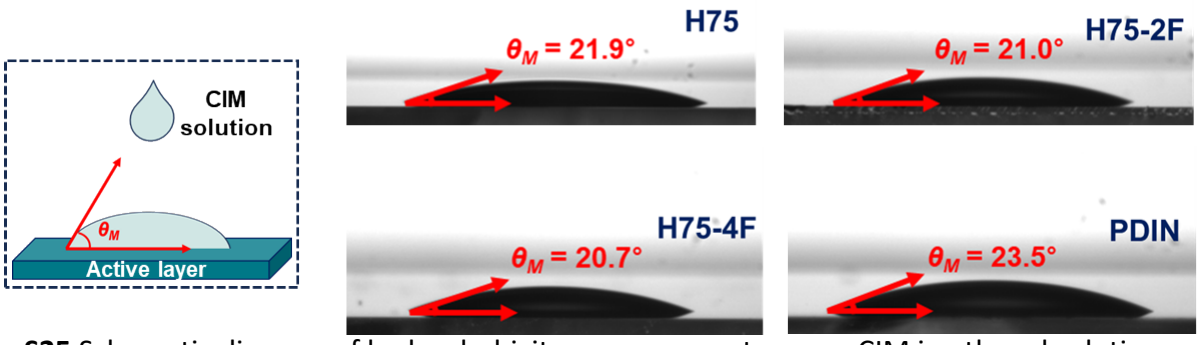

Fig. S25 Schematic diagram of hydrophobicity measurement among CIM in ethanol solutions on active layer films. The contact angle of H75, H75-2F, H75-4F, and PDIN on PM6: BTP-eC9 active layer film.

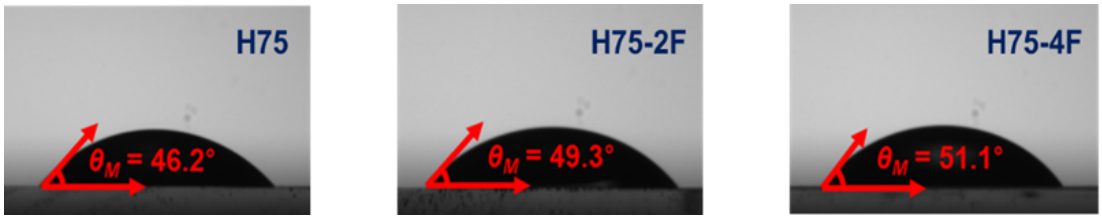

Fig. S26 The contact angle images of water on H75, H75-2F, and H75-4F CIM surfaces.

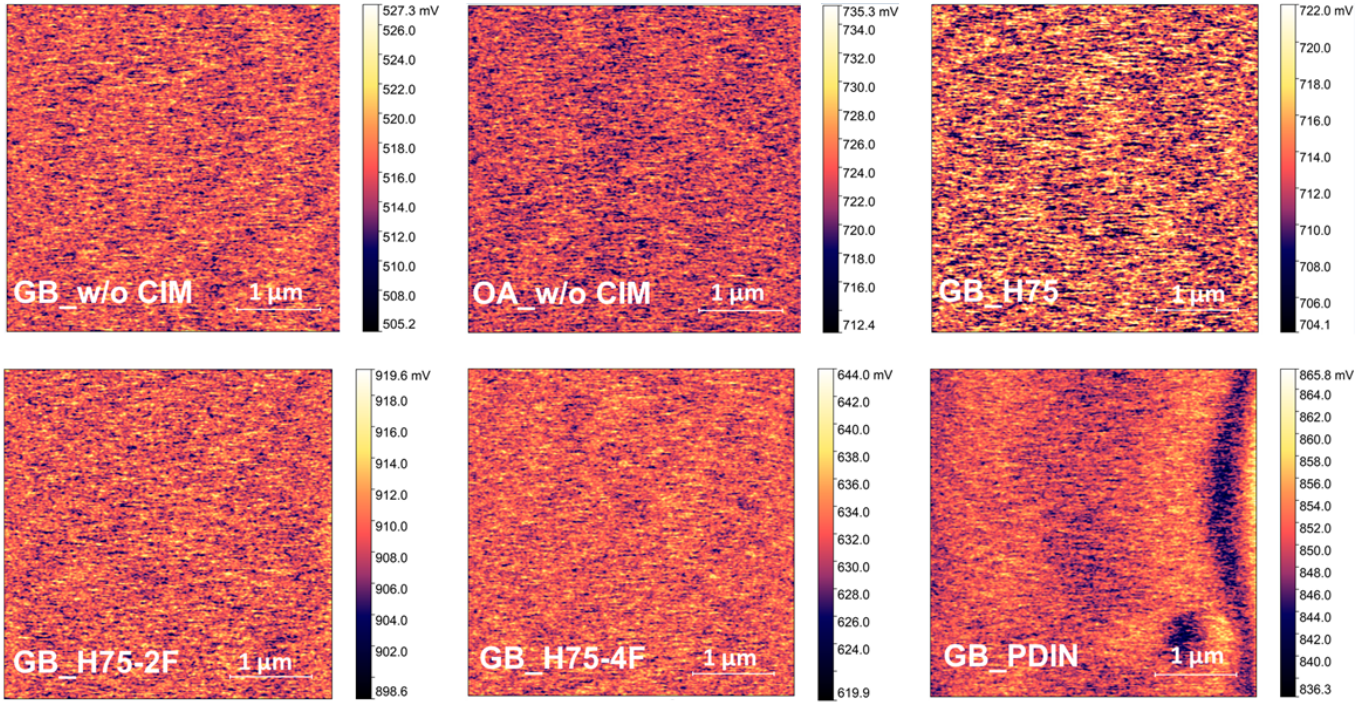

Fig. S27 The KPFM mapping of without and with H75, H75-2F, H75-4F, and PDIN CIM-deposited active layer films in GB and OA conditions.

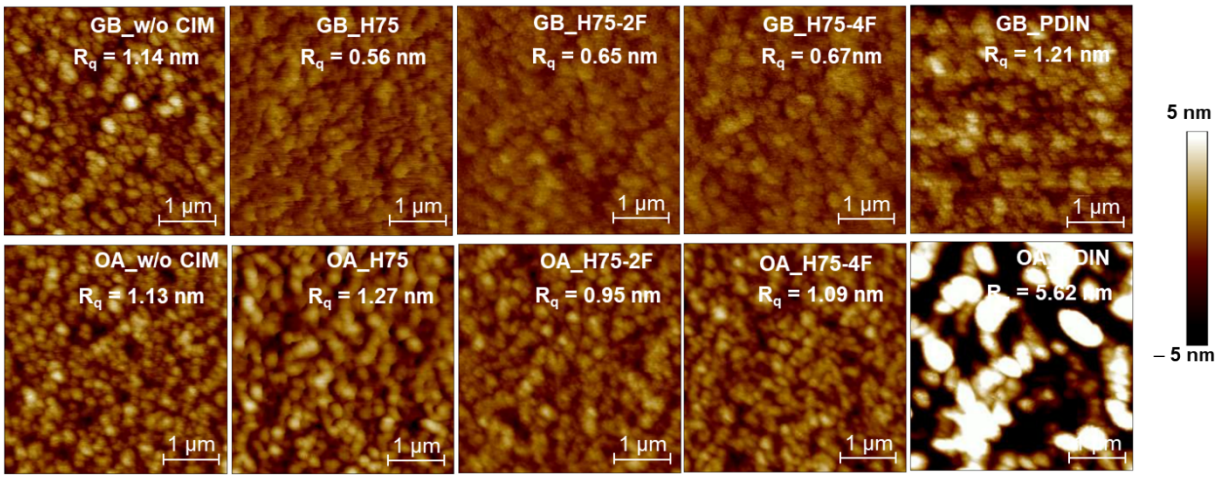

Fig. S28 AFM height images of active layer films without and with CIMs: H75, H75-2F, H75-4F, and PDIN, deposited under glovebox (GB) and open-air (OA) conditions.

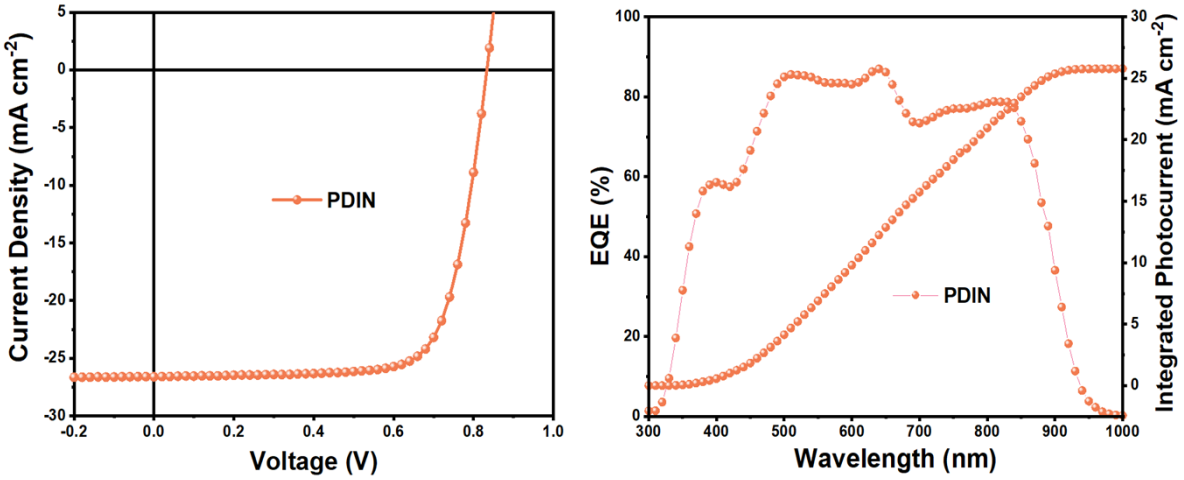

Fig. S29 The *J*–*V* and EQE curves of the PDIN-based device under GB conditions based on PM6:BTP-eC9 system with PDIN CIM.

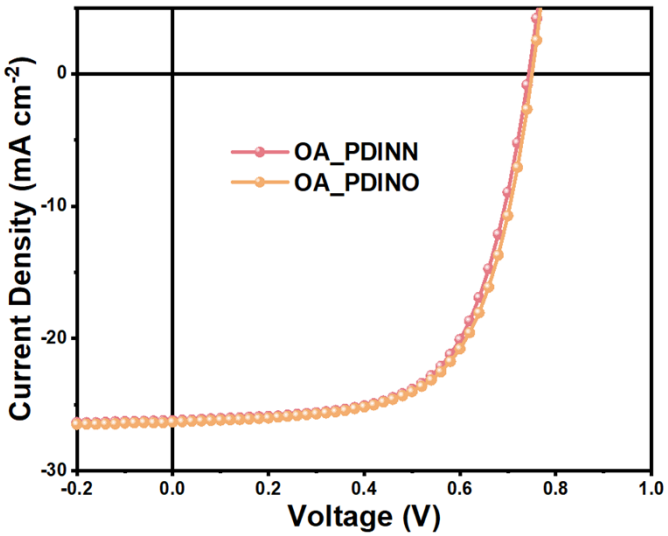

Fig. S30 The *J*–*V* curves of the OA and XY-processed devices based on PDINN and PDINO CIMs in ethanol solution on PM6:BTP-eC9 system under the illumination of AM 1.5G.

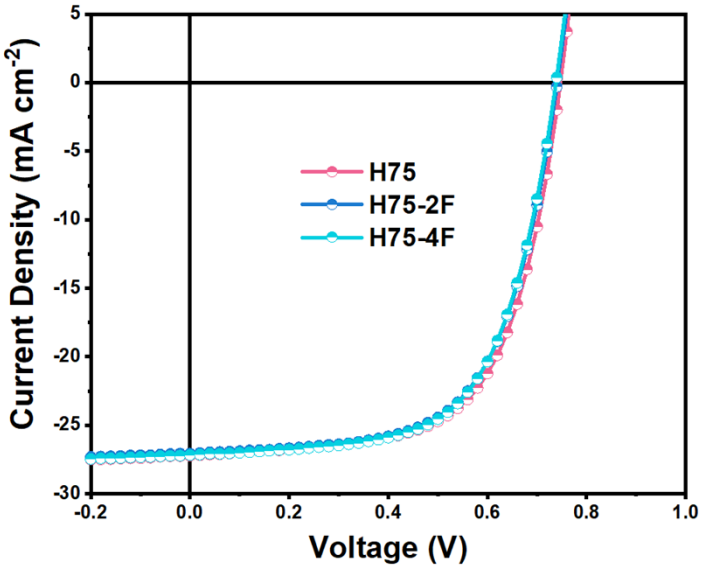

Fig. S31 The *J*–*V* curves of the OA and XY-processed devices based on H75, H75-2F, and H75-4F CIMs with the addition of acetic acid in ethanol solution on PM6:BTP-eC9 system under the illumination of AM 1.5G.

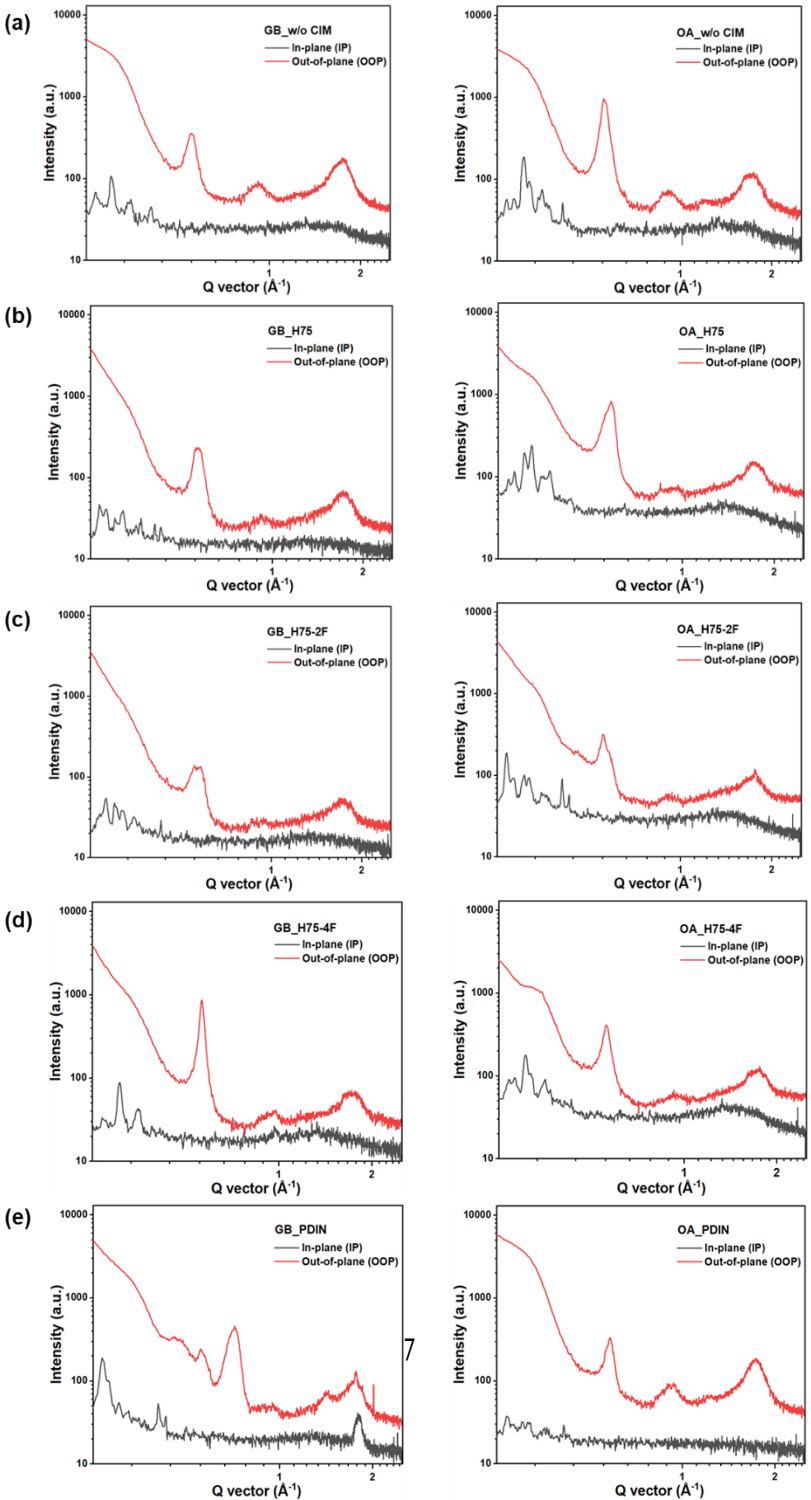

Fig. S32 1D GIWAXS line-cut profiles in the IP and OOP directions of (a) the active layer films without CIM, and with CIM deposited: (b) H75, (c) H75-2F, (d) H75-4F, and (e) PDIN, under GB and OA conditions.

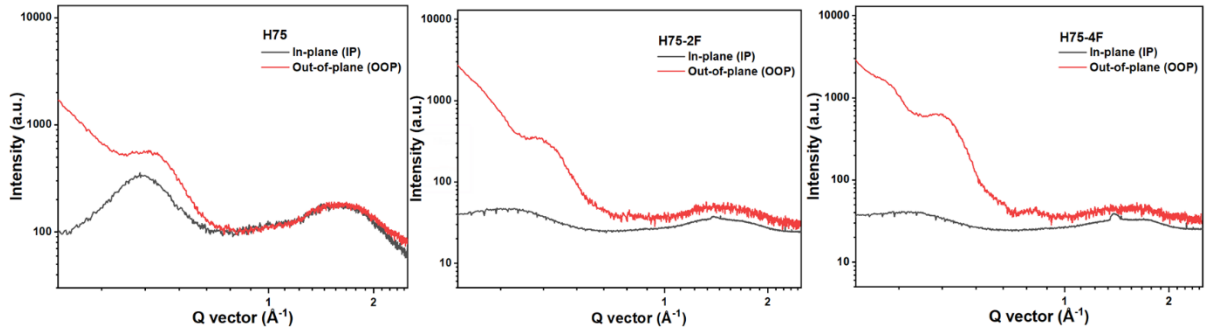

Fig. S33 1D GIWAXS line-cut profiles in the IP and OOP directions of H75, H75-2F, and H75-4F neat films.

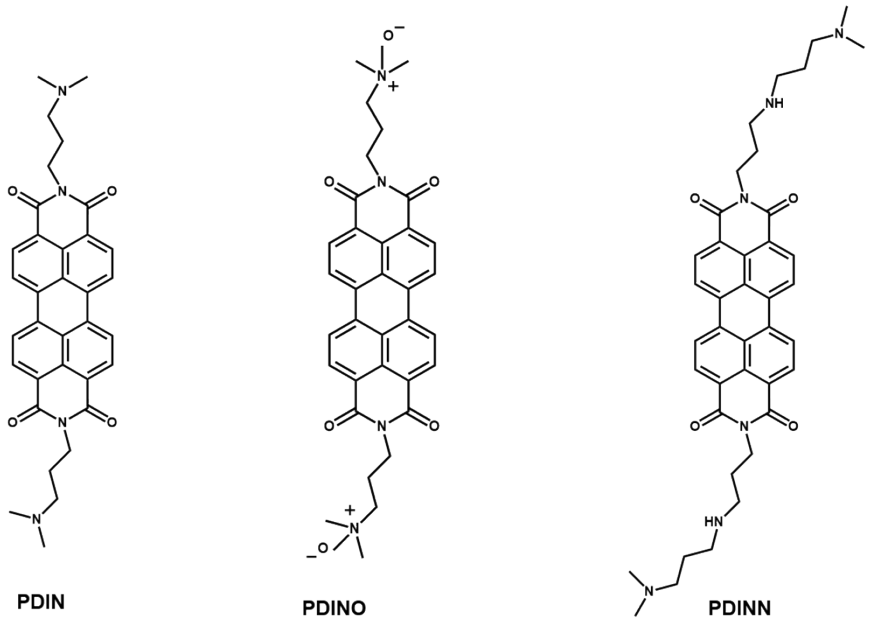

Fig. S34 The chemical structures of PDIN, PDINO, and PDINN CIMs.

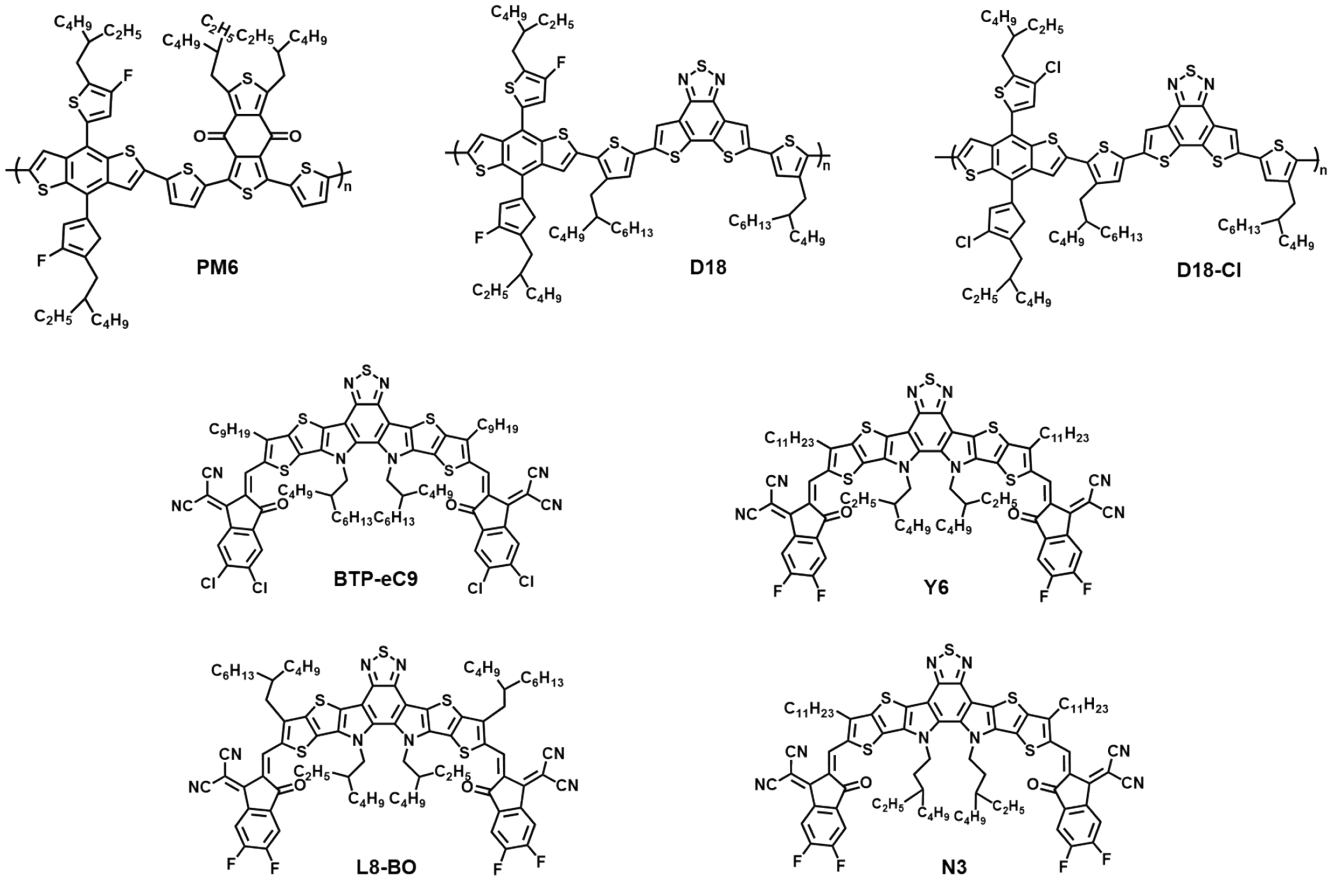

Fig. S35 Chemical structures of the active layer materials utilized in this work.

Table S1. The photovoltaic parameters ratio of devices based on H75, H75-2F, and H75-4F CIMs on PM6:BTP-eC9 under long-term stability in glovebox condition.

Time	CIMs	V_{OC} [a] (V)	PCE [a] (%)	FF [a] (%)	J_{SC} [a] (mA cm^{-2})
24 h	H75	1.00166	1.02246	1.00113	1.01954
	H75-2F	0.99174	1.03012	1.00314	1.03622
	H75-4F	0.99968	1.02003	1.00091	1.01941
120 h	H75	0.99815	1.0015	0.98604	1.0176
	H75-2F	0.9993	1.00971	0.99533	1.01515
	H75-4F	0.99261	0.99462	0.99119	1.01165
360 h	H75	0.99392	0.96797	0.95986	1.01449
	H75-2F	0.99287	0.99387	0.97898	1.02264
	H75-4F	0.97837	0.96046	0.97597	1.00589

864 h	H75	0.97521	0.9416	0.94516	1.02136
	H75-2F	0.9817	0.97283	0.98479	1.00633
	H75-4F	0.97124	0.90247	0.9241	1.00521
1080 h	H75	0.97483	0.86333	0.88103	1.00205
	H75-2F	0.96941	0.95409	0.95695	1.02843
	H75-4F	0.94715	0.83228	0.85071	1.02997

[a] the average PCE values are obtained from at least 10 cells.

Table S2. The photovoltaic parameters ratio of devices based on H75, H75-2F, and H75-4F CIMs on PM6:BTP-eC9 under light-soaking stability in glovebox condition.

Time	CIMs	V_{OC} (V)	V_{OC} [a]	PCE (%)	PCE [a]	FF [a]	FF [a]	J_{SC} (mA cm^{-2})	J_{SC} [a] (mA cm^{-2})
24 h	H75	0.95303	0.91182	0.87079	0.85095	0.94119	0.8953	0.97085	1.04228
	H75-2F	0.95743	0.94336	0.89148	0.92133	0.94769	0.93651	0.98248	1.04353
	H75-4F	0.93386	0.86973	0.80044	0.73659	0.89408	0.84216	0.95859	1.00557
48 h	H75	0.9329	0.91325	0.84056	0.8396	0.93595	0.90541	0.96259	1.01526
72 h	H75-2F	0.94767	0.94188	0.8702	0.90477	0.94521	0.94006	0.97154	1.02258
192 h	H75-4F	0.92684	0.87555	0.77012	0.72588	0.86434	0.84424	0.95964	0.98524
72 h	H75	0.94134	0.9114	0.82131	0.83075	0.89638	0.87142	0.9706	1.04572
312 h	H75-2F	0.93327	0.93661	0.83134	0.89555	0.90743	0.94227	0.97912	1.01577
	H75-4F	0.92939		0.72311		0.83378		0.93277	
432 h	H75	0.92728		0.77278		0.86623		0.96147	
	H75-2F	0.93367		0.80164		0.88248		0.9715	
	H75-4F	0.92086		0.71895		0.8191		0.9507	
552 h	H75	0.93308		0.74616		0.8409		0.95125	
	H75-2F	0.92156		0.79178		0.89784		0.95708	
	H75-4F	0.91208		0.68844		0.81619		0.92472	

[a] the average PCE values are obtained from at least 10 cells.

	H75-4F	0.87031	0.71685	0.82052	1.00367
96 h	H75	0.91036	0.82676	0.89373	1.01614
	H75-2F	0.94033	0.8858	0.9106	1.03526
	H75-4F	0.86651	0.71265	0.80599	1.02039
120h	H75	0.90946	0.80684	0.86805	1.02197
	H75-2F	0.92591	0.87392	0.91849	1.028
	H75-4F	0.83854	0.67369	0.79622	1.00897
144 h	H75	0.92511	0.78304	0.82993	1.02018
	H75-2F	0.91151	0.85474	0.9007	1.0414
	H75-4F	0.85874	0.67468	0.77885	1.00868
240 h	H75	0.90525	0.77987	0.83406	1.03286
	H75-2F	0.92722	0.84062	0.88577	1.02377
	H75-4F	0.81211	0.64104	0.77274	1.02138
336 h	H75	0.89945	0.70961	0.77055	1.02382
	H75-2F	0.90054	0.79037	0.8457	1.03812
	H75-4F	0.77625	0.58382	0.73982	1.01662
408 h	H75	0.8696	0.67289	0.7438	1.03782
	H75-2F	0.86881	0.71235	0.78386	1.0434
	H75-4F	0.72948	0.52895	0.70548	1.02495

Table S3. The photovoltaic parameters ratio of devices based on H75, H75-2F, and H75-4F CIMs on PM6:BTP-eC9 under air ambient environment stability(40–60 % RH, 25 ℃).
[a] the average PCE values are obtained from at least 10 cells.

Table S4. The photovoltaic parameters ratio of devices based on H75, H75-2F, and H75-4F CIMs on PM6:BTP-eC9 under thermal stress stability in glovebox condition.

Time	CIMs	V_{OC} [a] (V)	PCE [a] (%)	FF [a] (%)	J_{SC} [a] (mA cm^{-2})
24 h	H75	0.95089	0.92286	0.95727	1.01402
	H75-2F	0.9551	0.93903	0.97581	1.00759
	H75-4F	0.96317	0.89702	0.92967	1.00172
120 h	H75	0.92336	0.82522	0.89038	1.00413
	H75-2F	0.93207	0.85518	0.91841	0.99868
	H75-4F	0.90105	0.74927	0.85056	0.97928
240 h	H75	0.88929	0.79022	0.87791	1.0109
	H75-2F	0.91625	0.83274	0.91057	0.99825
	H75-4F	0.84084	0.63747	0.76274	0.99066
336 h	H75	0.89763	0.76792	0.86248	0.99232
	H75-2F	0.90594	0.7946	0.88689	0.98897
	H75-4F	0.83094	0.61772	0.76474	0.97159
456 h	H75	0.8901	0.73444	0.82581	0.99836
	H75-2F	0.89744	0.76065	0.83506	1.01302
	H75-4F	0.78684	0.52273	0.7008	0.94734

[a] the average PCE values are obtained from at least 10 cells

Table S5. PCE data of OSCs corresponding to plots in Fig. 3c.

Year	Type of structure	Systems	PCE (%)	Ref
2017	Inverted	PTB7-Th:PDI-DPP-PDI	5.6	[2]
	Conventional	POD2T-DTBT and PDTBT-alt-TT:PCBM	5.87	[3]
2018	Conventional	FTAZ:IT-M	9.1	[4]
			9.6	
			11.0	
2019	Conventional	PTzBI-Si:N2200	11.76	[5]
2020	Inverted	PM6:Y6	15.2	[6]
			15.6	
			15.4	
2021	Inverted	PM6:Y6	15.93	[7]
		PTB7-Th:IEICO-4F	11.10	[8]
		PM6:Y6	15.51	[9]
		PM6:Y6	15.91	[10]
			14.58	
			14.75	
2022	Inverted	PM6:Y6	15.03	[11]
			14.72	
			14.29	
	Conventional	PM6:Y6	15.10	[12]
		PM6:BTP-eC9	17.15	
2023	Inverted	PM6:Y6-hu	17.38	[13]
2024	Conventional	PM6:BTP-eC9	17.78	**This work**

Table S6. The photovoltaic parameters of the OA and XY-processed OSCs devices based on PDINN and PDINO as the CIM in ethanol solution on PM6:BTP-eC9 system under the illumination of AM 1.5G, 100 mW cm^{-2}

CIMs	V_{OC} [a] (V)	J_{SC} [a] (mA cm^{-2})	FF [a] (%)	PCE [a] (%)
PDINN	0.742 (0.740 ± 0.004)	26.44 (26.23 ± 0.19)	63.44 (62.69 ± 0.54)	12.45 (12.17 ± 0.17)
PDINO	0.749 (0.750 ± 0.0003)	26.58 (25.78 ± 0.12)	63.76 (63.72 ± 0.11)	12.69 (12.32 ± 0.05)

[a] the average PCE values are obtained from 5 cells.

Table S7. The photovoltaic parameters of the OA and XY-processed OSCs devices based on H75, H75-2F, and H75-4F as the CIM with the addition of acetic acid in ethanol solution on PM6:BTP-eC9 system under the illumination of AM 1.5G, 100 mW cm^{-2}

CIMs	V_{OC} [a] (V)	J_{SC} [a] (mA cm^{-2})	FF [a] (%)	PCE [a] (%)
H75	0.745 (0.742 ± 0.004)	27.21 (27.02 ± 0.38)	63.59 (62.56 ± 0.79)	12.90 (12.56 ± 0.38)
H75-2F	0.739 (0.739 ± 0.001)	27.56 (27.23 ± 0.26)	62.83 (62.35 ± 0.42)	12.82 (12.55 ± 0.16)
H75-4F	0.737 (0.734 ± 0.003)	27.17 (27.23 ± 0.50)	62.99 (61.14 ± 0.98)	12.61 (12.22 ± 0.31)

[a] the average PCE values are obtained from 5 cells.

7. Reference

1 T. L. H. Mai, S. Jeong, S. Kim, S. Jung, J. Oh, Z. Sun, J. Park, S. Lee, W. Kim and C. Yang, *Adv. Funct. Mater.*, 2023, **33**, 2303386.

2 S. M. McAfee, S. V. Dayneko, P. Josse, P. Blanchard, C. Cabanetos and G. C. Welch, *Chem. Mat.*, 2017, **29**, 1309-1314.

3 S.-L. Lim, K.-H. Ong, J. Li, L. Yang, Y.-F. Chang, H.-F. Meng, X. Wang and Z.-K. Chen, *Org. Electron.*, 2017, **43**, 55-63.

4 L. Ye, Y. Xiong, Q. Zhang, S. Li, C. Wang, Z. Jiang, J. Hou, W. You and H. Ade, *Adv. Mater.*, 2018, **30**, 1705485.

5 L. Zhu, W. Zhong, C. Qiu, B. Lyu, Z. Zhou, M. Zhang, J. Song, J. Xu, J. Wang, J. Ali, W. Feng, Z. Shi, X. Gu, L. Ying, Y. Zhang and F. Liu, *Adv. Mater.*, 2019, **31**, 1902899.

6 H. Zhao, H. B. Naveed, B. Lin, X. Zhou, J. Yuan, K. Zhou, H. Wu, R. Guo, M. A. Scheel, A. Chumakov, S. V. Roth, Z. Tang, P. Müller-Buschbaum and W. Ma, *Adv. Mater.*, 2020, **32**, 2002302.

7 J. Yuan, D. Liu, H. Zhao, B. Lin, X. Zhou, H. B. Naveed, C. Zhao, K. Zhou, Z. Tang, F. Chen and W. Ma, *Adv. Energy Mater.*, 2021, **11**, 2100098.

8 N. Chaturvedi, N. Gasparini, D. Corzo, J. Bertrandie, N. Wehbe, J. Troughton and D. Baran, *Adv. Funct. Mater.*, 2021, **31**, 2009996.

9 Y. Li, H. Liu, J. Wu, H. Tang, H. Wang, Q. Yang, Y. Fu and Z. Xie, *ACS Appl. Mater. Interfaces*, 2021, **13**, 10239-10248.

10 R. Ma, T. Yang, Y. Xiao, T. Liu, G. Zhang, Z. Luo, G. Li, X. Lu, H. Yan and B. Tang, *Energy Environ. Mater.*, 2022, **5**, 977-985.

11 J. Xue, H. B. Naveed, H. Zhao, B. Lin, Y. Wang, Q. Zhu, B. Wu, Z. Bi, X. Zhou, C. Zhao, K. Zhou and W. Ma, *J. Mater. Chem. A*, 2022, **10**, 13439-13447.

12 H. Li, S. Liu, X. Wu, Q. Qi, H. Zhang, X. Meng, X. Hu, L. Ye and Y. Chen, *Energy Environ. Sci.*, 2022, **15**, 2130-2138.

13 S. Rasool, J. W. Kim, H. W. Cho, Y.-J. Kim, D. C. Lee, C. B. Park, W. Lee, O.-H. Kwon, S. Cho and J. Y. Kim, *Adv. Energy Mater.*, 2023, **13**, 2203452.